Cell

Wnt Signaling Requires Sequestration of Glycogen Synthase Kinase 3 inside Multivesicular Endosomes

Vincent F. Taelman,[1,3] Radoslaw Dobrowolski,[1,3] Jean-Louis Plouhinec,[1] Luis C. Fuentealba,[1,4] Peggy P. Vorwald,[1] Iwona Gumper,[2] David D. Sabatini,[2] and Edward M. De Robertis[1,*]

[1]Howard Hughes Medical Institute and Department of Biological Chemistry, University of California, Los Angeles, Los Angeles, CA 90095-1662, USA

[2]Department of Cell Biology, New York University School of Medicine, New York, NY 10016-6497, USA

[3]These authors contributed equally to this work

[4]Present address: Department of Neurological Surgery, University of California, San Francisco, San Francisco, CA 94143-0525, USA

*Correspondence: ederobertis@mednet.ucla.edu

DOI 10.1016/j.cell.2010.11.034

SUMMARY

Canonical Wnt signaling requires inhibition of Glycogen Synthase Kinase 3 (GSK3) activity, but the molecular mechanism by which this is achieved remains unclear. Here, we report that Wnt signaling triggers the sequestration of GSK3 from the cytosol into multivesicular bodies (MVBs), so that this enzyme becomes separated from its many cytosolic substrates. Endocytosed Wnt colocalized with GSK3 in acidic vesicles positive for endosomal markers. After Wnt addition, endogenous GSK3 activity decreased in the cytosol, and GSK3 became protected from protease treatment inside membrane-bounded organelles. Cryoimmunoelectron microscopy showed that these corresponded to MVBs. Two proteins essential for MVB formation, HRS/Vps27 and Vps4, were required for Wnt signaling. The sequestration of GSK3 extended the half-life of many other proteins in addition to β-Catenin, including an artificial Wnt-regulated reporter protein containing GSK3 phosphorylation sites. We conclude that multivesicular endosomes are essential components of the Wnt signal-transduction pathway.

INTRODUCTION

Canonical Wnt signaling plays a crucial role in development, tissue regeneration, stem cells, and cancer (Logan and Nusse, 2004; Clevers, 2006; MacDonald et al., 2009; Angers and Moon, 2009). A cytoplasmic destruction complex consisting of Glycogen Synthase Kinase 3 (GSK3, which has α and β isoforms), Casein Kinase 1 (CK1), Adenomatous Polyposis Coli (APC), and Axin mediates the phosphorylation of β-Catenin. Phosphorylation targets β-Catenin for polyubiquitinylation and subsequent degradation in proteasomes. In the presence of Wnt, the destruction complex becomes inactivated in ways that are incompletely understood. Wnt triggers signaling by binding to Frizzled and LDL-receptor related protein 6 (LRP6), causing the aggregation of Dishevelled (Dvl) and Axin on the plasma membrane (Bilic et al., 2007; Zeng et al., 2008). The key step in the canonical pathway is the inactivation of GSK3, as evidenced by the fact that pharmacological inhibition of this enzyme elicits a typical Wnt signal. The molecular mechanism of GSK3 inhibition remains one of the main open questions in the Wnt field (Wu and Pan, 2010).

Internalization of receptor complexes is an absolute requirement for Wnt signaling (Blitzer and Nusse, 2006; Yamamoto et al., 2006). Bilic et al. (2007) discovered that cytoplasmic particles designated LRP6-signalosomes—containing aggregates of phospho-LRP6, Frizzled, Dvl, Axin, and GSK3—are formed at and under the plasma membrane 15 min after Wnt addition. Activated Wnt receptors recruit Axin and GSK3, which phosphorylates five critical PPPS/TP sequences in the intracellular domain of LRP6 (Zeng et al., 2008; Niehrs and Shen, 2010). A number of mechanisms have been proposed to explain the inhibition of GSK3 (Kimelman and Xu, 2006). For example, the LRP6 tail may act as a direct inhibitor of GSK3 (Mi et al., 2006; Cselenyi et al., 2008; Piao et al., 2008; Wu et al., 2009). The LRP6 PPPSP repeats serve both as substrates and binding sites for GSK3 and may act as competitive inhibitors of this enzyme, although at low affinity (K_i of 1.3×10^{-5} M; Cselenyi et al., 2008).

GSK3 has many substrates in addition to β-Catenin, including Dvl, Axin, and APC (Jope and Johnson, 2004). This promiscuous enzyme phosphorylates serine or threonine at position −4 of sites primed by phosphorylation (S/TXXXS/T[PO_3]) (Cohen and Frame, 2001). We reported that the transcription factor Smad1 is polyubiquitinylated and degraded after GSK3 phosphorylation and is stabilized by canonical Wnt signaling, resulting in the integration of BMP and Wnt signaling (Fuentealba et al., 2007). Additional substrates destabilized by GSK3 phosphorylation have since been identified (Kim et al., 2009).

During our investigations on signaling integration, we measured GSK3 enzyme activity in Wnt-treated cell extracts (prepared in the presence of Triton X-100) and were surprised to find that Wnt did not change GSK3 activity (data not shown),

even though in the direct GSK3 inhibition model one would have predicted inhibition. How could this be? Upon reflection, we realized that following ligand binding and endocytosis, growth factor receptors are incorporated into multivesicular endosomes within 15 min (Gruenberg and Stenmark, 2004). Multivesicular body (MVB) formation is an obligatory step before degradation in lysosomes can take place (Katzmann et al., 2002). As first discovered for EGF receptor, the topology is such that the cytoplasmic side of the plasma membrane corresponds to the lumen of the small MVB vesicles (McKanna et al., 1979). Therefore, Wnt-induced MVB formation would cause GSK3 bound to phosphorylated LRP6 cytoplasmic tails (and other GSK3 substrates such as Axin, APC, β-Catenin, and Dvl) to become sequestered from its cytosolic substrates by two layers of membrane (see model in Figure 7), effectively inhibiting its activity.

In this study, we tested the GSK3 sequestration hypothesis of Wnt signaling. Fluorescence microscopy showed that Wnt signaling caused the relocalization of cytoplasmic GSK3 to vesicles that colocalized with endocytosed xWnt8-Venus protein, and with the MVB and lysosomal markers Rab7 and LysoTracker. Wnt signal transduction was blocked by depletion of Hrs/Vps27 or expression of dominant-negative Vps4, two proteins essential for intralumenal vesicle formation in MVBs (Katzmann et al., 2002; Wollert and Hurley, 2010). Moreover, Wnt treatment decreased cytosolic GSK3 activity levels (measured in Digitonin-permeabilized cells), yet full enzyme activity was recovered after solubilization of all membranes with Triton X-100. Similarly, Wnt caused endogenous GSK3β to become partially protected from Proteinase K digestion, but only in the absence of Triton X-100. Finally, cryoimmunoelectron microscopy showed that GSK3 was indeed translocated from the cytosol into MVBs after Wnt pathway activation. Bioinformatic analyses revealed that 20% of the human proteome contains multiple putative GSK3 phosphorylation sites. Total protein half-life was extended by Wnt treatment or GSK3 inhibition. The addition of GSK3 phosphorylation sites was sufficient to place the stability of a Green Fluorescent Protein (GFP) biosensor under the control of Wnt. We conclude that canonical Wnt signaling sequesters GSK3 inside MVBs, reducing its cytosolic levels and extending the half-life of many GSK3 substrates.

RESULTS

Wnt Causes GSK3 Relocalization in Acidic Cytoplasmic Vesicles

We first asked whether Wnt treatment changed the subcellular localization of GSK3. Human 293T cells expressing xWnt8-Venus (Mii and Taira, 2009) were cultured together with mouse 3T3 cells transfected with GSK3-RFP. Remarkably, endocytosed Wnt-Venus and GSK3-RFP accumulated in the same vesicular structures (arrows in Figure 1F), while GSK3-RFP levels decreased in the cytosol (Figures 1A–1F). Relocalization of endogenous GSK3β was also observed in these cocultures (Figures S1A–S1C available online). Wnt-Venus puncta were counted in each responding cell (n = 80), and 56% ± 9% of them colocalized with GSK3-RFP puncta (see histogram in Figure 1C′). Thus, cytosolic GSK3 decreases and becomes relocalized to the same endosomes as the internalized Wnt ligand.

Transfection of constitutively active LRP6 lacking its extracellular domain, designated CA-LRP6, causes a potent Wnt signal (Tamai et al., 2004) . CA-LRP6 cytoplasmic signalosome formation (Bilic et al., 2007) required Dynamin and caused a striking relocalization of GSK3β from the cytosol into prominent cytoplasmic puncta (Figures 1G–1L′ and Figures S1D–S1O). Treatment of 3T3 cells with LysoTracker, a dye that becomes concentrated in acidic organelles such as MVBs and lysosomes, showed that endogenous GSK3β relocated to these compartments (Figure 1G–1L′). In addition, GSK3β colocalized with Dvl, Axin, and LysoTracker, as well as the PI3P probe FYVE-GFP, when Wnt signaling was activated by overexpression of Dvl (Figures S2A–S2O). Remarkably, a protein consisting of the DIX domain of Dvl fused to the LRP6 cytoplasmic tail (DIX > Ctail-GFP), which triggers a very strong Wnt signal (Metcalfe et al., 2010), also formed signalosomes colocalizing with acidic vesicles that sequestered cytosolic GSK3β (Figures S2P–S2Aa).

CA-LRP6 signalosomes colocalized with the late endosomal marker Rab7-GFP (Figures 1M–1R) in 62% ± 7% of the GSK3 puncta, indicating that GSK3-RFP relocated to MVBs or lysosomes (Bucci et al., 2000). About 40% of GSK3-RFP vesicles colocalized with Vps4-GFP (see Figures 3L–3N′), a marker of the final stages of intralumenal vesicle formation in endosomes (Bishop and Woodman, 2000; Gruenberg and Stenmark, 2004). In untransfected 3T3 cells the number and size of endogenous GSK3β puncta increased after treatment with Wnt3a conditioned medium (Figures 1S–1U) in cells permeabilized with Digitonin (which facilitates the visualization of intracellular organelles; Bishop and Woodman [2000]).

Taken together, these results strongly support the hypothesis that Wnt signaling causes the relocalization of cytosolic GSK3 to the endosomal compartment.

GSK3 Is Sequestered inside MVBs

To determine whether Wnt3a treatment sequesters GSK3 kinase activity from cytosol, endogenous cytosolic kinase activity was measured in untransfected L cells permeabilized with Digitonin through the incorporation of phosphate from [γ^{32}P]-ATP into a phospho-glycogen synthase peptide substrate (Ryves et al., 1998). Digitonin solubilizes cholesterol-rich patches in the plasma membrane, leaving MVBs and other intracellular organelles intact (Dunn and Holz, 1983). Addition of Wnt3a for 4 hr decreased cytosolic GSK3 activity levels by 66% ± 5% (Figure 2A, lanes 1 and 2), and the missing GSK3 activity was recovered when all membranes were dissolved with 0.1% Triton X-100 (Figure 2A, compare lanes 2 and 4).

The gold standard to determine the localization of a protein inside a membrane-bounded compartment is the protease protection assay. GSK3 protein became protected from Proteinase K digestion (Vanlandingham and Ceresa, 2009) after Wnt3a treatment (Figure 2B, compare lanes 3 and 4) in untransfected L cells permeabilized with Digitonin. This Wnt-dependent protease protection of GSK3 was eliminated when membranes were solubilized with 0.1% Triton X-100 (Figure 2B, lanes 4 and 6). As a negative control, we used α-tubulin, which is not contained in vesicular organelles and was not protected from Proteinase K digestion (Figure 2B). These experiments strongly

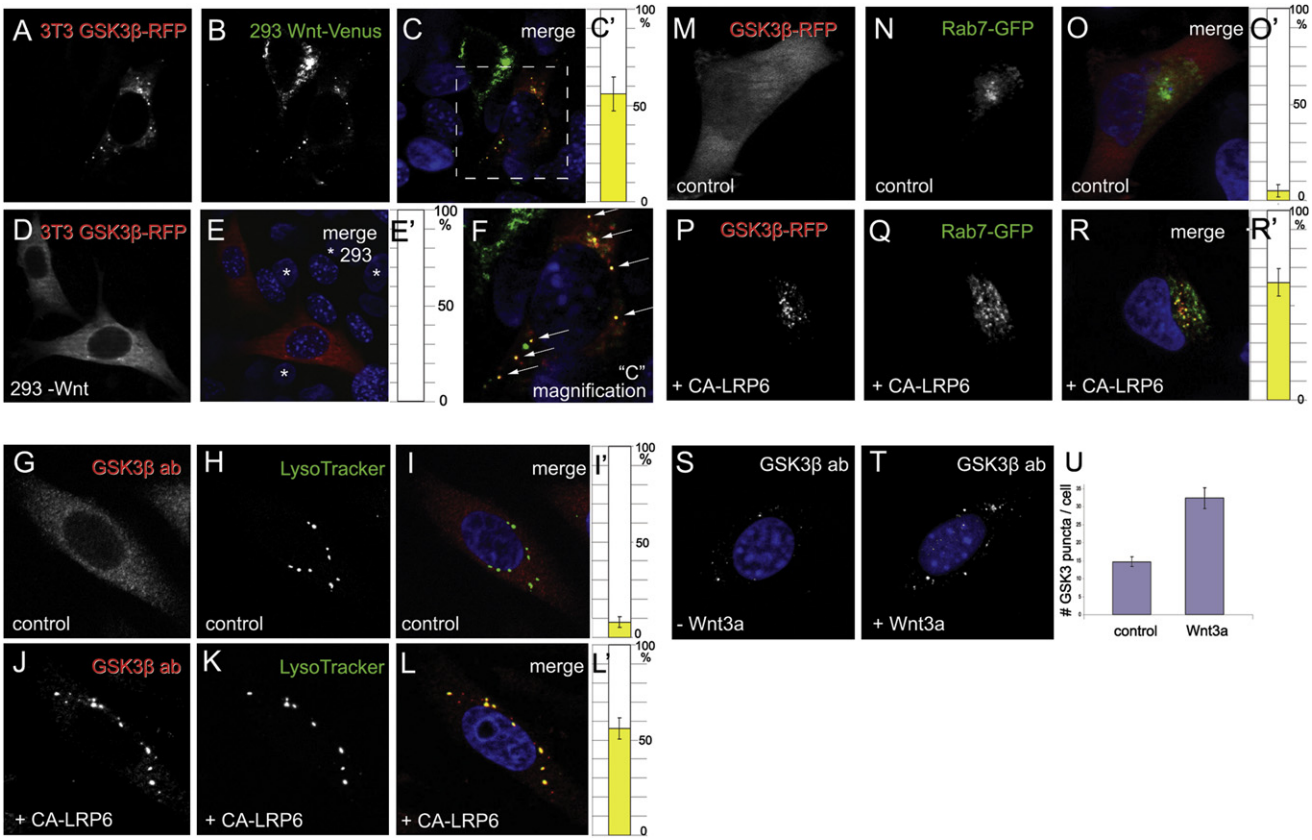

Figure 1. GSK3β Is Translocated to Acidic Vesicles upon Wnt Signaling

(A–F) In coculture experiments, xWnt8-Venus (green) secreted by 293T cells caused the relocalization of GSK3β-RFP (red) in 3T3 cells that endocytosed Wnt. Arrows in the enlargement in (F) indicate xWnt8-Venus endosomes that sequester GSK3-RFP. In controls lacking xWnt8-Venus, GSK3-RFP localization was cytoplasmic (D and E); asterisks indicate untransfected control 293 cell nuclei.

(G–L′) GSK3β antigen relocalized to LysoTracker-positive endosomes upon activation of Wnt pathway by CA-LRP6 in 3T3 cells; note that endogenous GSK3β was depleted from cytoplasm.

(M–R′) Rab7-GFP (green) and GSK3β-RFP (red) colocalized in CA-LRP6 signalosomes (in 62% ± 7% of GSK3-positive puncta, n = 80 HeLa cells); note GSK3 sequestration from cytosol.

(S–U) Endogenous GSK3β puncta (white) were larger and more numerous after 4 hr of Wnt3a addition to untransfected 3T3 cells permeabilized with Digitonin. Data are represented as mean ± SEM. Also see Figure S1 and Figure S2.

suggest that GSK3 becomes sequestered within membrane-bounded organelles upon Wnt treatment.

The relocalization of GSK3 to multivesicular endosomes in Wnt3a-treated cells was visualized by cryoimmunoelectron microscopy. In untransfected 3T3 cells treated with control conditioned medium, endogenous GSK3β was found almost exclusively in the cytosol, whereas in Wnt3a-treated cells a substantial fraction was found inside MVBs (Figures 2C and 2D). In HeLa cells cotransfected with CA-LRP6 and GSK3-GFP, an anti-GFP antibody revealed colloidal Gold particles in MVBs (Figure 2E). In some cases Gold particles were observed on the cytoplasmic surface of vesicles fusing with multivesicular endosomes (Figure 2F), as well as within the small vesicles that fill MVBs (arrows with asterisks in Figure 2F), supporting the topology shown in Figure 7. In the absence of CA-LRP6, Gold-labeled GSK3-GFP was located in the cytosol (Figure 2G).

To confirm the cryoimmuno localization results in a quantitative way, we resorted to an activated mutant of Rab5. Rab5-Q79L causes the formation of giant multivesicular endosomes containing large numbers of intralumenal vesicles (Wegener et al., 2010). These MVBs are so large that the outer membrane (outlined by Rab5-QL-DsRed) can be readily distinguished from its internal contents by light microscopy. As shown in Figures 2H–2M, GSK3β translocated from the cytoplasm into the interior of Rab5-QL multivesicular endosomes (arrows, 77% ± 9% colocalization) when CA-LRP6 was coexpressed, but not in its absence. Cytosolic depletion of GSK3-GFP was very clear (compare Figures 2J and 2M).

Taken together, these results demonstrate that the GSK3 enzyme becomes translocated from the cytosol into membrane-bounded multivesicular endosomes when Wnt signals.

Wnt Signaling Requires the ESCRT Machinery

The molecular machinery that forms endosomal intralumenal vesicles has been well characterized (Wollert and Hurley, 2010). Several endosomal sorting complexes required for

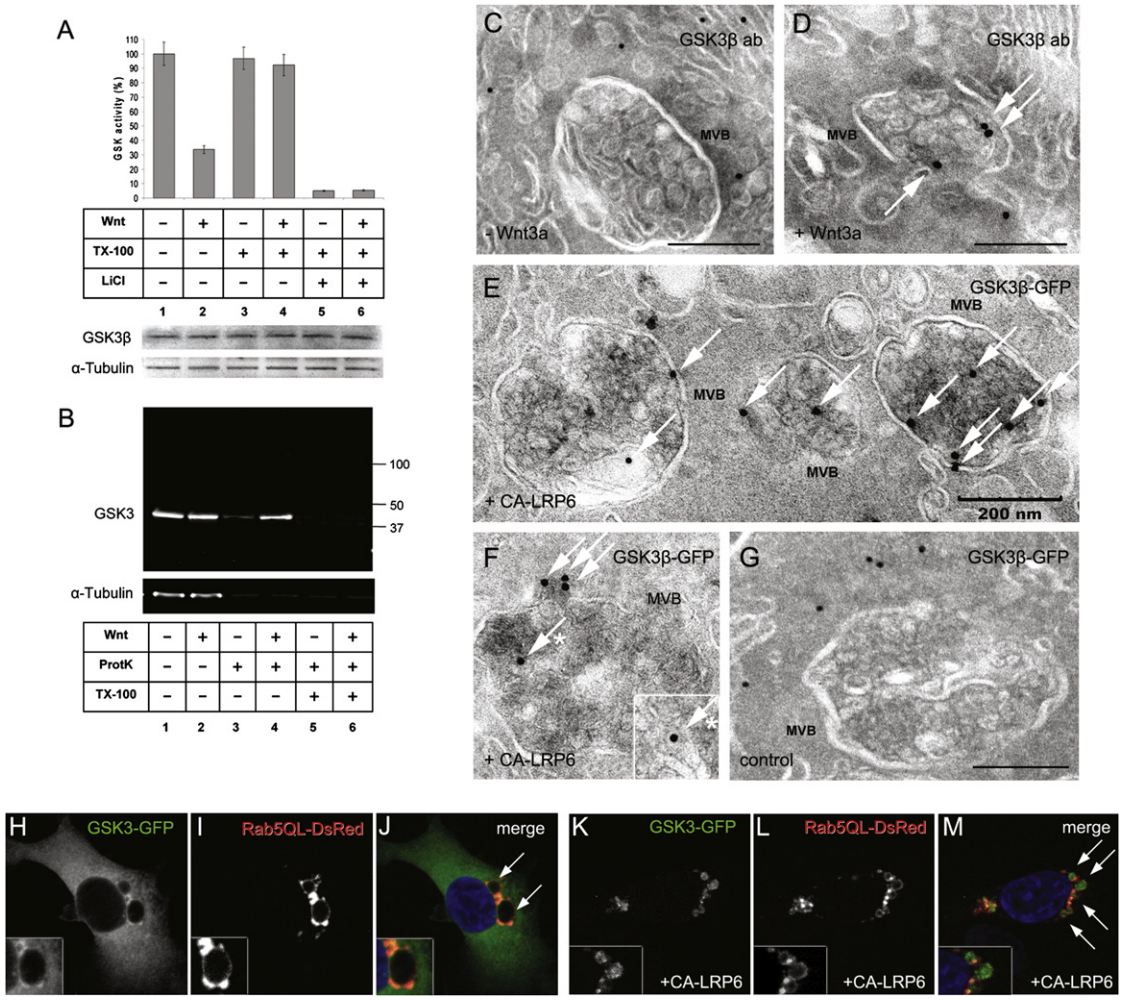

Figure 2. Wnt Signaling Causes Sequestration of GSK3 inside Multivesicular Endosomes

(A) GSK3 kinase activity was decreased by 66% ± 5% by Wnt3a treatment and was recovered after membrane solubilization with 0.1% Triton X-100 in Digitonin-permeabilized L cells. LiCl inhibition shows that the radioactive assay was specific for GSK3. Data are from two independent experiments using untransfected L cells. GSK3β and α-tubulin provide loading controls.

(B) GSK3β becomes protected from Proteinase K after Wnt3a treatment, but only in the absence of Triton X-100 (lanes 3–6). Similar results were obtained in five independent experiments (untransfected L cells). All samples were permeabilized with Digitonin, which causes leakage of 37% of the endogenous GSK3 (three independent experiments).

(C and D) Cryoimmunoelectron microscopy demonstrating relocation of endogenous GSK3β into MVBs (arrows) after Wnt3a treatment in untransfected 3T3 cells.

(E–G) GSK3-GFP localized in MVBs (white arrows) in CA-LRP6 transfected HeLa cells but was cytosolic in control cells lacking CA-LRP6 transfection.

(H–J) Rab5-QL-DsRed forms giant endosomes (arrows), whereas GSK3β-GFP remains uniformly distributed in the cytosol (n = 100).

(K–M) In the presence of CA-LRP6, GSK3-GFP is translocated inside Rab5-QL giant multivesicular endosomes (see arrows) in 77% ± 9%, n = 80, of cotransfected cells. Note that GSK3 becomes depleted from cytosol.

Data are represented as mean ± SEM.

transport, or ESCRTs, have been identified through yeast genetics (designated Vacuolar Protein Sorting, Vps, mutants) and biochemistry (Katzmann et al., 2002). The GSK3 sequestration hypothesis predicts that ESCRT proteins essential for vesicle invagination should be required for Wnt signaling. Therefore, we tested two ESCRT proteins essential for vesicle formation (Figure 3A).

HRS/Vps27 (hepatocyte growth factor regulated tyrosine-kinase substrate) initiates formation of the ESCRT-0 complex. Depletion of HRS by siRNA blocked the accumulation of β-Catenin observed after 2 hr of Wnt3a treatment in 293T cells, whereas control scrambled siRNA had no effect (Figure 3B, lanes 1–4). Total GSK3 levels increased by about 70% when HRS was depleted (Figure 3B compare lanes 1 and 3, three independent experiments; see also Figure S3), suggesting that GSK3 is normally partially degraded by the endosomal machinery; however, Wnt addition did not significantly change GSK3 levels in these experiments. We were expecting a decrease in total

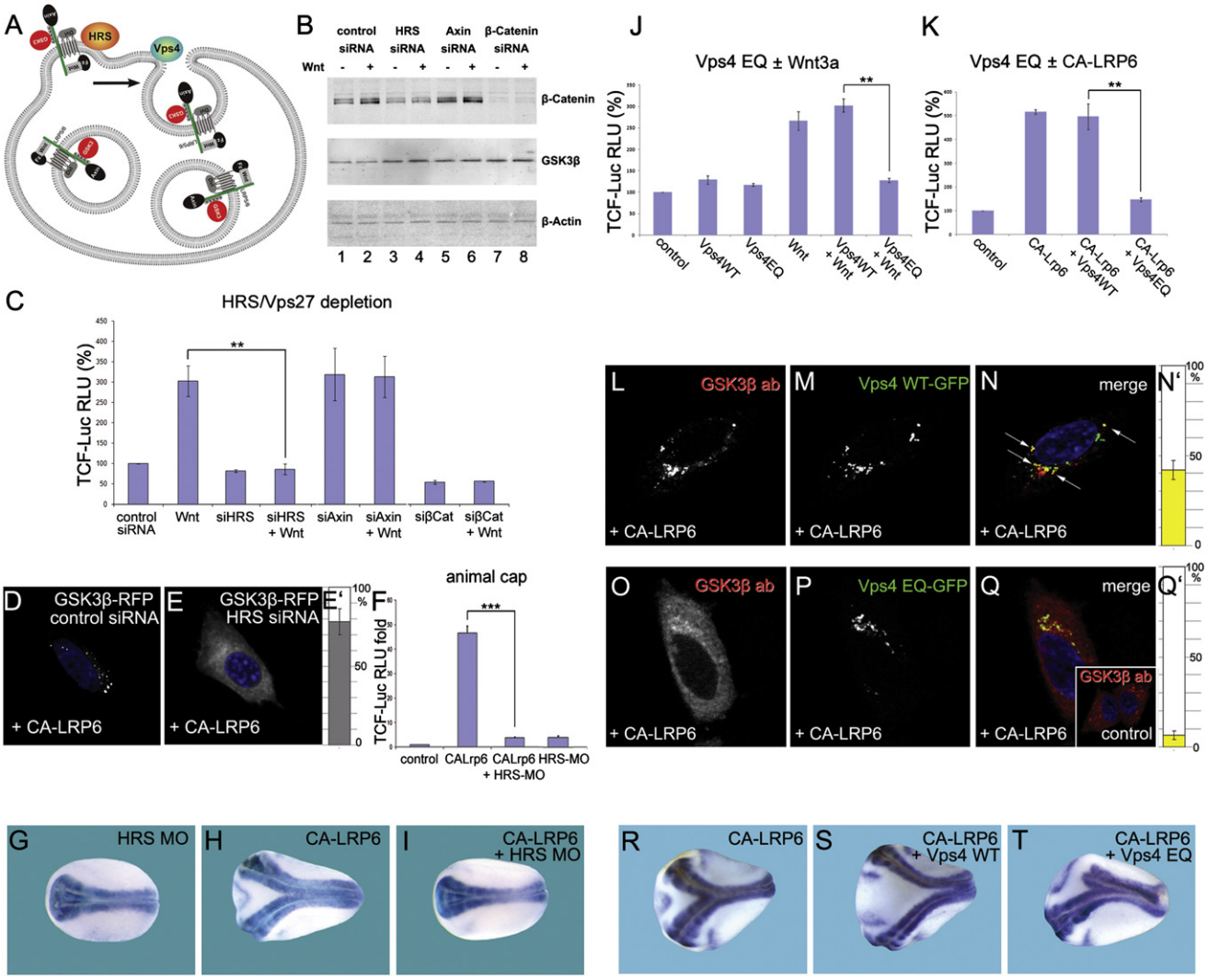

Figure 3. Components of the ESCRT Machinery Are Required for Wnt Signaling

(A) HRS and Vps4 are proteins required for intralumenal vesicle formation in MVBs. GSK3 is indicated in red.

(B) HRS siRNA inhibits Wnt3a-induced accumulation of β-Catenin.

(C) TCF-Luciferase reporter gene assays showing that Wnt signaling requires HRS (brackets).

(D–E′) HRS is required for sequestration of GSK3-RFP in CA-LRP6 signalosomes (78% ± 8%, n = 150).

(F) Wnt signaling induced by *CA-LRP6* mRNA in *Xenopus* animal caps was blocked by HRS morpholino (brackets). (G–I) Induction of secondary axis in *Xenopus* embryos by *CA-LRP6* mRNA (80 pg) requires HRS (neural tissue visualized with *Sox2* probe).

(J and K) Expression of Vps4-EQ, but not Vps-WT, inhibited signaling by Wnt3a or CA-LRP6 (brackets) in 293T cells.

(L–N′) CA-LRP6 signalosomes sequestered endogenous GSK3β and partly colocalized with Vps4-WT-GFP, a multivesicular endosome marker (43% ± 5% of vesicles, arrows, in n = 80 cells).

(O–Q′) Overexpression of Vps4-EQ-GFP inhibits sequestration of endogenous GSK3β in CA-LRP6 signalosomes. (R–T) Head formation in axes induced by CA-LRP6 was inhibited by *Vps4-EQ*, but not by *Vps4-WT* mRNA.

Data are represented as mean ± SEM. Also see Figure S3 and Figure S4.

GSK3 levels in western blots because MVBs are usually targeted to the lysosome and degradation. Many reasons might explain this result. For example GSK3 may have a long half-life, it may be replenished by translational regulation, or GSK3 may have a long time of residency in MVBs induced by Wnt signaling before lysosomal degradation takes place (Wnt might even affect the rate of MVB processing globally). In addition there is recent evidence that intralumenal MVB vesicles may be recycled back into the cytosol by "back-fusion" to the late endosome-limiting membrane (Falguieres et al., 2009). Despite the lack of change in total levels, the relocation of GSK3 from the cytosol into MVBs is clearly documented in the figures above, providing the basis for the sequestration model for Wnt signaling presented in Figure 7.

The requirement of HRS for Wnt signal transduction was demonstrated directly in these cultures by measuring the expression of the SuperTopFlash-Luciferase reporter, which contains multiple TCF-binding sites (Figure 3C, brackets). In addition we observed that relocalization of GSK3 into vesicle-like structures in CA-LRP6 transfected cells was blocked by HRS siRNA and was not affected by control scrambled siRNA (Figures 3D–3E′). In animal cap explants the activation of TCF-Luciferase by *CA-LRP6* mRNA was blocked by HRS antisense morpholino (Figure 3F, brackets). In *Xenopus* embryos, injection of *CA-LRP6* mRNA into a single ventral blastomere at the eight-cell stage caused complete axis duplications, which were eliminated by coinjection of HRS MO (Figures 3G–3I and Figure S4N). HRS depletion did not affect cell viability or proliferation until neurula stage (Figures S4A–S4M). The effects of HRS MO could be partially rescued by human *HRS* mRNA (Figures 4C and 4O).

Vps4 is an ATPase required for the disassembly of ESCRT-III complexes, the last step in the pinching off of intralumenal vesicles in multivesicular endosomes (Gruenberg and Stenmark, 2004). A point mutation in the ATPase site (Vps4-EQ) creates a potent dominant-negative form that inhibits MVB formation (Bishop and Woodman, 2000). Vps4-EQ blocked canonical Wnt3a signaling (Figure 3J, brackets). The control in this experiment was Vps4-WT, which differs by only one amino acid yet was without effect in TCF-Luciferase assays. Vps4-EQ also inhibited the transcriptional effects of CA-LRP6 (Figure 3K, brackets). Vps4-EQ cotransfection inhibited the relocalization of endogenous cytosolic GSK3β into CA-LRP6 signalosomes (Figures 3L–3Q). In *Xenopus* embryos, *Vps4-EQ*, but not *Vps4-WT*, coinjected with CA-LRP6 mRNA into a ventral blastomere inhibited the formation of complete secondary axes containing head structures (Figures 3R–3T and Figure S4O). Importantly, we also tested the requirement of the ESCRT machinery for axis induction by Siamois, a homeobox gene activated by Wnt signaling. We found that *Vps4-EQ* mRNA was unable to inhibit Siamois secondary axes (see Figures 4Ba–4Da and Figure S5A). This epistatic experiment placed the requirement for Vps4 early in the Wnt pathway, upstream of its transcriptional effector Siamois.

These experiments show that two components of the ESCRT machinery, HRS/Vps27 and Vps4, are required for canonical Wnt signaling.

β-Catenin Is Required for GSK3 Sequestration

While investigating the requirements for GSK3 sequestration, we made an unexpected finding: the translocation of GSK3 into CA-LRP6 signalosomes and its depletion from the cytosol were inhibited by β-Catenin siRNA (Figures 4A and 4B and Figure S3C). Using SuperTopFlash reporter in animal caps, we found that HRS MO blocked signaling by microinjected *β-Catenin* mRNA and was partially rescued by human *HRS* mRNA coinjection (Figure 4C). We also noticed that endogenous β-Catenin, especially its GSK3-phosphorylated form (i.e., targeted for degradation), colocalized with CA-LRP6-GFP in signalosomes (Figures 4D–4F). Taken together, these results suggest that β-Catenin is required for the sequestration of GSK3 in multivesicular endosomes.

We next asked whether β-Catenin overexpression was sufficient to trigger GSK3 sequestration in endosomes. Stabilized β-Catenin-GFP (in which its three GSK3 sites were mutated into alanines) accumulated in the nucleus as expected but also in cytoplasmic vesicle-like structures, which sequestered GSK3-RFP (Figures 4G–4I). Wild-type β-Catenin-GFP accumulated inside giant Rab5-QL MVBs (Figures 4J–4L) and in LysoTracker-positive vesicles (Figures S3D–S3F). Injection of *β-Catenin* mRNA into a ventral cell causes twinning in *Xenopus* embryos. Coinjection of *β-Catenin* mRNA with HRS-MO or Vps4-EQ showed that MVB formation was required for β-Catenin axis induction in *Xenopus* (Figures 4M–4R and Figures S4P and S4Q).

This new function of β-Catenin in sequestering GSK3 in MVBs occurs upstream of the well-established transcriptional role of β-Catenin and Tcf3 in Wnt signaling (Clevers, 2006). Depletion of β-Catenin with MO generated ventralized *Xenopus* embryos lacking all neural structures (Figures 4S and 4T). Although GSK3 inhibition by *DN-GSK3β* mRNA (a dominant-negative catalytically inactive form) greatly expanded neural structures, this effect was blocked by β-Catenin or xTcf3 depletion (Figures 4U–4W). However, a construct fusing the transactivation domain of *Xenopus* β-Catenin to DN-xTcf3 was able to signal in β-Catenin-depleted embryos (Figure 4X). In secondary axis induction assays, the β-Catenin-DN-xTcf3 fusion was active even when MVB formation was inhibited by *Vps4-EQ* mRNA microinjection (Figures 4Y–4Aa and Figure S5B). These experiments show that the classical transcriptional role of β-Catenin/Tcf3 is distinct from its new function in facilitating GSK3 sequestration.

We conclude that β-Catenin protein is required and sufficient to cause GSK3 sequestration in acidic cytoplasmic endosomes. It has been proposed that the entire destruction complex (which includes β-Catenin) is recruited to phosphorylated LRP6 receptors (Zeng et al., 2008). Once β-Catenin levels begin to rise during Wnt signaling, β-Catenin would enhance the signal, forming a feed-forward loop by facilitating GSK3 sequestration.

Sequestration of GSK3 Regulates Protein Half-Life

Phosphorylation of β-Catenin or Smad1 by GSK3 causes recognition by E3 polyubiquitin ligases and protein degradation (Logan and Nusse, 2004; Fuentealba et al., 2007). To investigate whether GSK3 sequestration causes the stabilization of other proteins in addition to β-Catenin and Smad1, we first designed computer algorithms to identify potential phosphate-primed GSK3 sites in the human proteome (Figure 5A) and whether they were evolutionary conserved. A large number of proteins (20% of the proteome) were found to contain three or more consecutive potential GSK3 sites (Table S1 and Table S3), significantly more than expected from random distribution (Table S1). These included many novel putative GSK3 targets with known regulatory functions (Table S2).

To determine whether Wnt/GSK3 signaling regulates overall protein stability, we carried out radioactive pulse-chase experiments with ^{35}S methionine in untransfected 293T cells. Cultured cells were radioactively labeled for 30 min, washed, and then treated with Wnt3a or control conditioned medium containing a 4-fold excess of unlabeled methionine. As shown in Figure 5B, the total half-life of labeled cellular proteins increased from 9.3 to

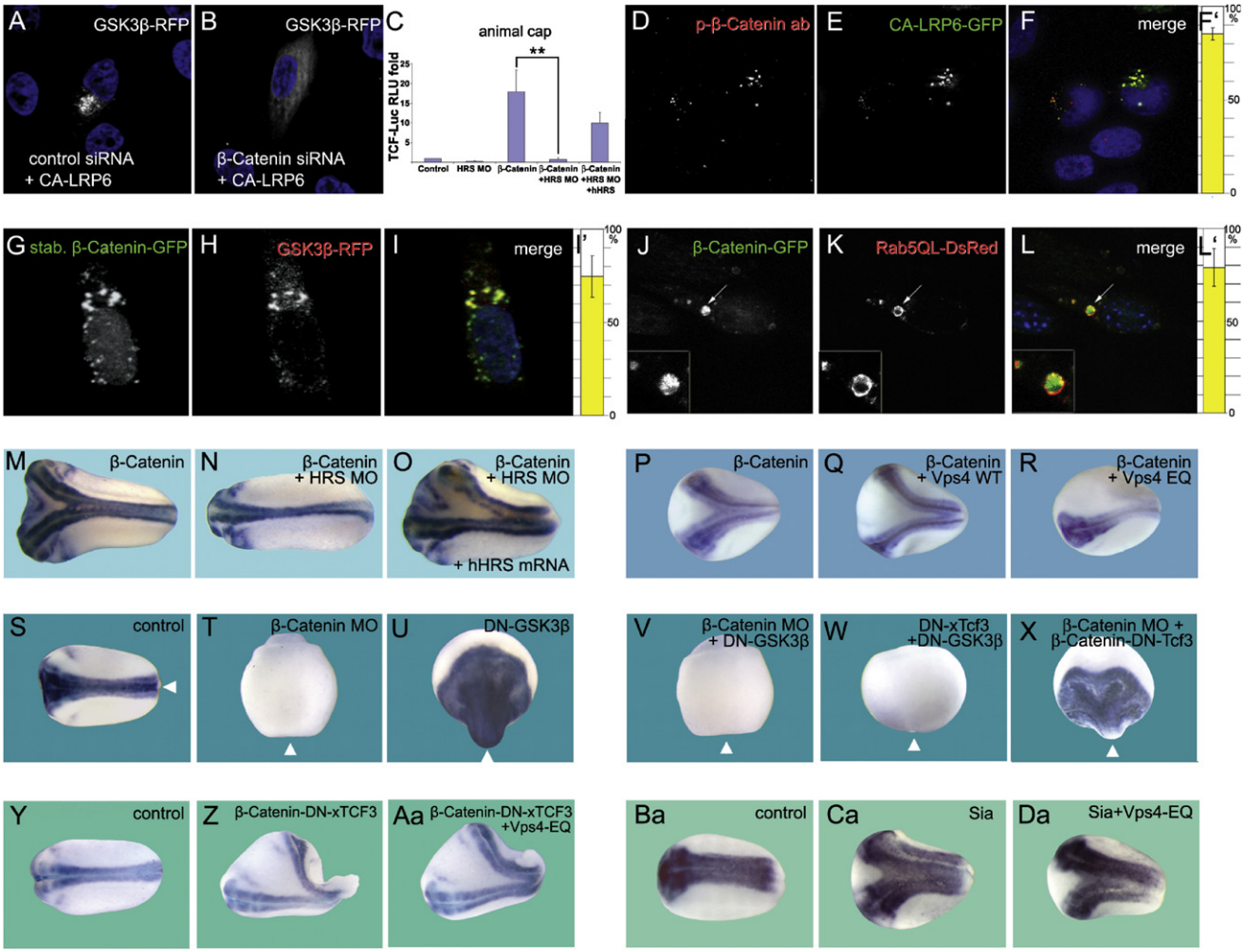

Figure 4. β-Catenin Is Required for GSK3 Localization in Multivesicular Endosomes

(A and B) β-Catenin siRNA inhibited GSK3β relocalization in CA-LRP6 signalosomes (in 86% ± 7% of transfected HeLa cells, n = 300).

(C) HRS MO blocks the induction of TCF reporter expression (brackets) by *β-Catenin* mRNA (four injections of 80 pg) in *Xenopus* animal cap explants, and this was partially rescued by human *HRS* mRNA.

(D–F′) Endogenous phospho-β-Catenin colocalizes with CA-LRP6-GFP signalosomes in HeLa cells (85% ± 3% of transfected cells, n = 56).

(G–I′) Overexpression of a stabilized mutant of β-Catenin-GFP caused its accumulation both in the nucleus and in cytoplasmic particles that sequester GSK3-RFP from the cytoplasm (75% ± 11%, n = 60).

(J–L′) Wild-type β-Catenin-GFP becomes localized inside giant endosomes induced by Rab5-QL-DsRed. Seventy-nine percent ± 10% of giant MVBs contained β-Catenin-GFP, n = 80.

(M–O) Axis induction by *β-Catenin* mRNA (80 pg) in *Xenopus* was blocked by coinjection of HRS-MO and partially rescued by 10 pg human *HRS* mRNA.

(P–R) *Vps4-EQ*, but not *Vps4-WT*, mRNA inhibited secondary axis formation by *β-Catenin* mRNA.

(S–X) Nuclear function of β-Catenin in *Xenopus* embryos. Wild-type, but not β-Catenin depleted embryos, contains neural tissue marked by Sox2 (n = 44 and n = 25). Microinjection of *DN-GSK3* mRNA (150 pg, four times at four-cell) dorsalized in a β-Catenin dependent manner (n = 38 and n = 28). *DN-Tcf3* mRNA (200 pg, four times) blocked dorsalization by DN-GSK3 (n = 36), whereas the fusion construct β-Catenin-DN-xTcf3 (30 pg) rescued the ventralizing effects of β-Catenin MO (n = 26). Arrowheads indicate position of the blastopore.

(Y–Aa) Epistatic experiment showing that β-Catenin-DN-xTcf3 fusion protein does not require MVB formation to induce secondary axes in *Xenopus* embryos.

(Ba–Da) Epistatic experiment showing that the downstream target of Wnt signaling Siamois is not affected by MVB inhibition.

Data are represented as mean ± SEM. Also see Figure S5.

11.8 hr in Wnt3a medium. Electrophoresis and autoradiography after 6 hr of cold chase showed that a wide range of proteins were stabilized by Wnt treatment (Figure 5C, lanes 1 and 2), even when protein synthesis was inhibited with cycloheximide (Figure 5C, lanes 3 and 4; Figure S6A). Thus, the effect of Wnt on radioactive protein stability is direct and not due to the expression of genes activated after Wnt is added.

Wnt-stabilized proteins were detected mostly in the 35–150 kDa range (Figures 5D and 5F). The stabilization of radioactive proteins by Wnt was eliminated by depletion of β-Catenin

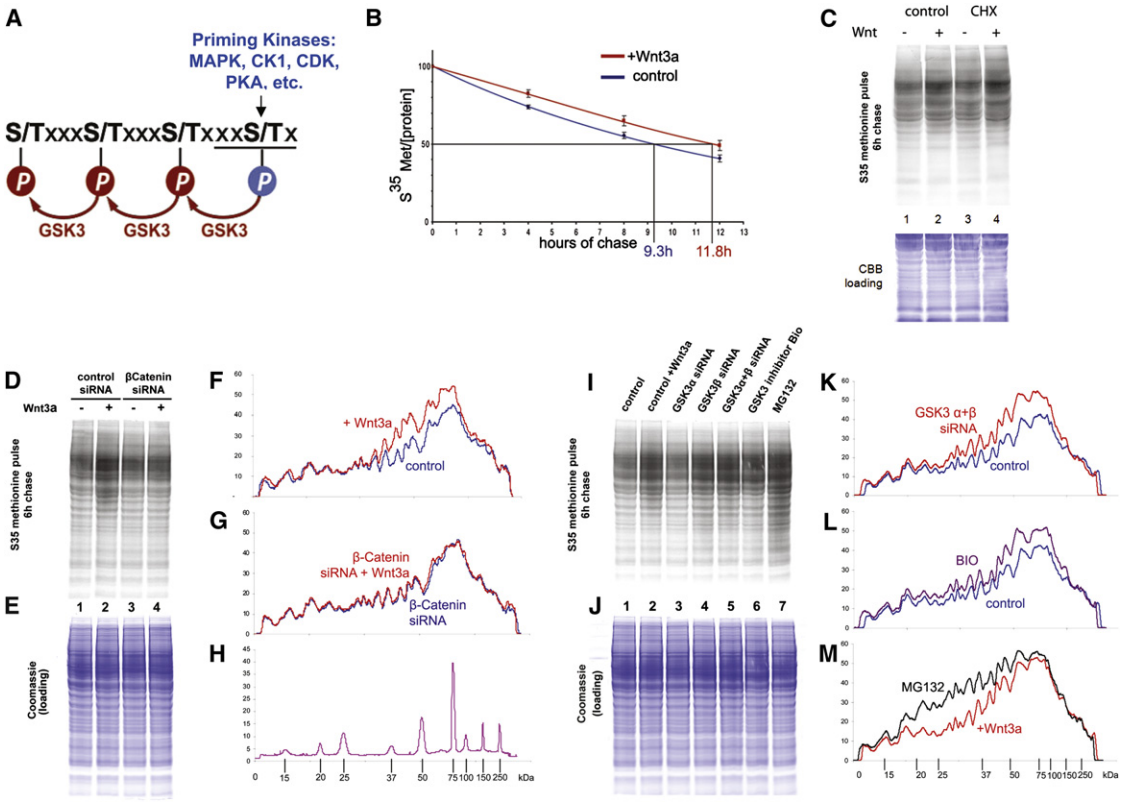

Figure 5. Wnt Prolongs the Half-Lives of Cellular Proteins via GSK3 Inhibition

(A) Twenty percent of human proteins contain three or more putative GSK3 sites primed by various kinases.

(B) Radioactive pulse-chase experiment showing that the half-life of total proteins was increased by Wnt3a treatment of 293T cells.

(C) Wnt3a treatment stabilized many proteins after 6 hr of chase in autoradiographs, even after inhibiting protein synthesis with cycloheximide (see Figure S6A); Coomassie brilliant blue (CBB) staining provides equal loading control.

(D–H) β-Catenin was required for protein stabilization by Wnt3a. Densitometric tracings show that proteins stabilized by Wnt are within the 35–150 kDa range (note m.w. standards).

(I–M) Depletion of GSK3α/β or their chemical inhibition by BIO resulted in protein stabilization similar to Wnt3a, whereas proteasomal inhibition by MG132 stabilized a wider range of proteins than Wnt3a or GSK3 inhibition.

Also see Figure S6, Table S1, Table S2, and Table S3.

with siRNA (Figures 5D–5H). This requirement for β-Catenin in protein stabilization is explained by our finding that β-Catenin is essential for the sequestration of GSK3 (Figure 4). Axin is required for LRP6 signalosome formation and signaling (Bilic et al., 2007) and also for overall protein stabilization by Wnt (Figure S6F).

Protein stabilization by Wnt3a mimicked the effects of GSK3 inhibition. In 293T cells, depletion of GSK3α had little effect on protein stability, but depletion of GSK3β, or GSK3α and β, stabilized the same range of proteins as Wnt3a treatment (Figure 5I, lanes 1–5). A chemical inhibitor of GSK3, BIO, caused a similar stabilization, whereas the proteasome inhibitor MG132 generated a different profile in which proteins below the 35 kDa range were also strongly stabilized (Figures 5I–5M). Thus, although Wnt signaling stabilized many proteins, these represented only a subset of the total proteome.

These results suggest that Wnt signaling and GSK3 activity are regulators of the half-life of many cellular proteins. Some of the novel putative GSK3 targets listed in Table S2, HDAC4 and JunB, were tested and found to be stabilized by Wnt treatment (Figures S6B–S6E). In addition the half-life of Smad4 was also regulated by Wnt, resulting in increased TGFβ signaling (H. Demagny and E.M.D.R., unpublished data). Testing all possible Wnt/GSK3 targets would be a daunting task, so we took a different approach, generating an artificial protein that serves as a biosensor of Wnt/GSK3activity.

A Reporter Protein for GSK3 Activity

What would be the effect of adding GSK3 sites to a protein that lacked them? An artificial GFP construct was generated in which three GSK3 sites primed by a canonical MAPK phosphorylation site (PXSP) were added to its carboxy-terminus via a row of alanines (Figure 6A). A Flag-tag and a PPAY site for the binding of E3 polyubiquitin ligases of the HECT family (mimicking Smad1; Fuentealba et al. [2007]) were also added. The HECT E3 ligase site helped but was not essential (Figure S7B); even in its absence, the biosensor protein could be destabilized by another E3 ligase, βTrcp (Figure S7C).

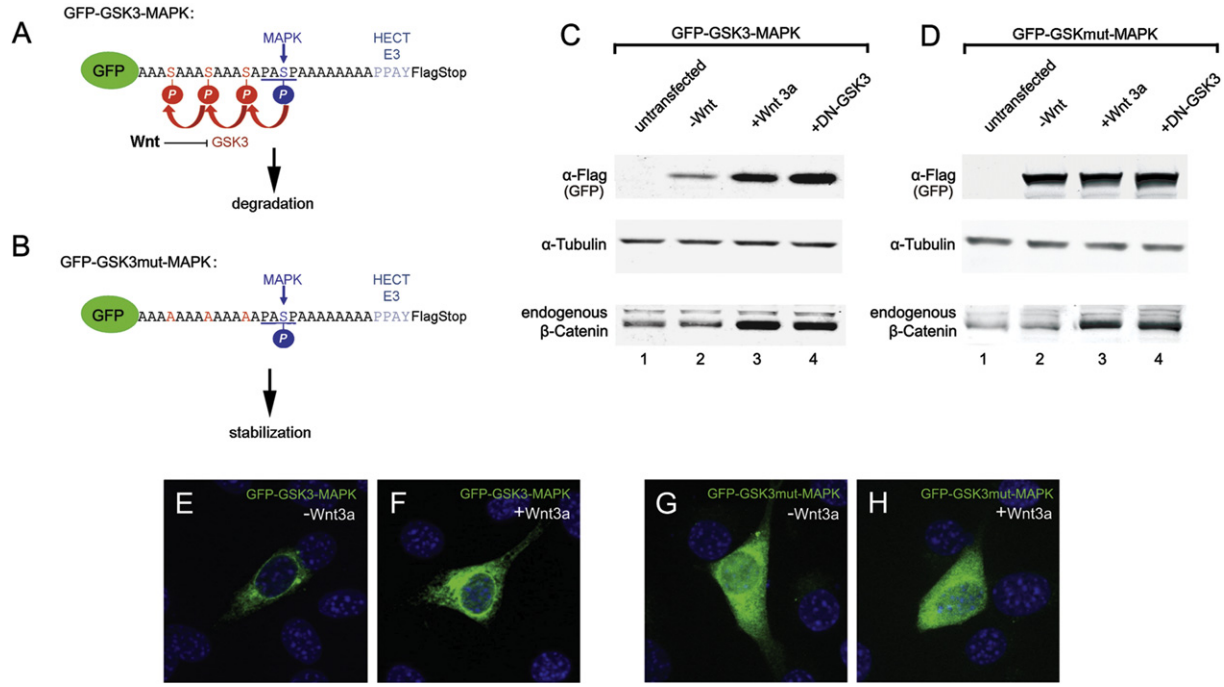

Figure 6. A Wnt-Regulated Reporter Protein Generated by Introducing Multiple GSK3 Phosphorylation Sites

(A and B) Sequences of the GFP-GSK3-MAPK biosensor construct and its GSK3 phosphorylation-resistant mutant. This protein is predicted to be primed by MAPK/Erk and further phosphorylated by GSK3.

(C) Western blot showing stabilization of GFP-GSK3-MAPK and endogenous β-Catenin by Wnt3a treatment (6 hr) or DN-GSK3 transfection in transfected 3T3 cells. α-Tubulin served as loading control.

(D) When GSK3 sites were mutated, GFP was stabilized and did not respond to Wnt.

(E–H) GFP fluorescence in 3T3 cells transfected with GFP reporter proteins. Note that fluorescence was increased by Wnt3a treatment or mutation of GSK3 sites. Also see Figure S7.

Cells were transfected with GFP-GSK3-MAPK construct, split into two cultures, and treated with control or Wnt3a conditioned medium for 6 hr. The GFP-GSK3-MAPK reporter protein was stabilized by Wnt3a treatment (Figure 6C, compare lanes 2 and 3,Figures 6E and 6F). Remarkably, the degree of stabilization of this biosensor protein was comparable to that of endogenous β-Catenin, whereas α-tubulin remained unchanged (Figure 6C). The stabilization caused by Wnt could be mimicked by cotransfection of DN-GSK3 (Figure 6C, lane 4) or by treatment with the GSK3 inhibitor BIO (data not shown). To demonstrate that stabilization by Wnt indeed occurred at a posttranslational level, we mutated the GSK3 sites into alanines, generating GFP-GSK3mut-MAPK (Figure 6B). This GSK3 phosphorylation-resistant protein became stabilized and was no longer affected by Wnt3a treatment (Figures 6D, 6G, and 6H). Thus, the presence of GSK3 phosphorylation sites is sufficient to destabilize GFP. The type of priming kinase was not critical because constructs primed by CK1 were similarly stabilized by Wnt (Figure S7E).

These studies with a GFP reporter protein indicate that multiple consecutive GSK3 phosphorylation sites make a protein less stable, presumably by favoring recognition by E3 polyubiquitin ligases of the βTrcp or HECT types (Logan and Nusse, 2004; Fuentealba et al., 2007). The results indicate that Wnt signaling is able to deplete GSK3 from the cytosol to levels low enough to stabilize a biosensor of cellular GSK3 activity. Because the proteome contains a multitude of GSK3 phosphorylation targets, we expect that canonical Wnt signaling will have many previously unsuspected metabolic effects.

DISCUSSION

We investigated the cellular mechanism by which Wnt signaling causes GSK3 inhibition. The results support a new model for canonical Wnt signal transduction, in which the GSK3 enzyme becomes sequestered inside multivesicular endosomes triggered by activation of the Frizzled and LRP6 receptors, decreasing GSK3 levels in the cytosol (Figure 7). The key insight that led to the GSK3 sequestration hypothesis was the realization that during the normal endocytosis process, early endosomes containing activated receptors are packaged within multivesicular endosomes (McKanna et al., 1979; Katzmann et al., 2002; Gruenberg and Stenmark, 2004). GSK3 is recruited to the cytoplasmic side of Wnt receptor complexes and phosphorylates LRP6 and other substrates such as Dvl, APC, Axin, and β-Catenin (MacDonald et al. [2009]; Table S2), to which it normally binds. The key to transcriptional activation by Wnt signaling is the nuclear accumulation of β-Catenin. Although β-Catenin protein initially translocates into MVBs together with GSK3, once cytosolic levels of GSK3 are sufficiently depleted, newly translated β-Catenin is not

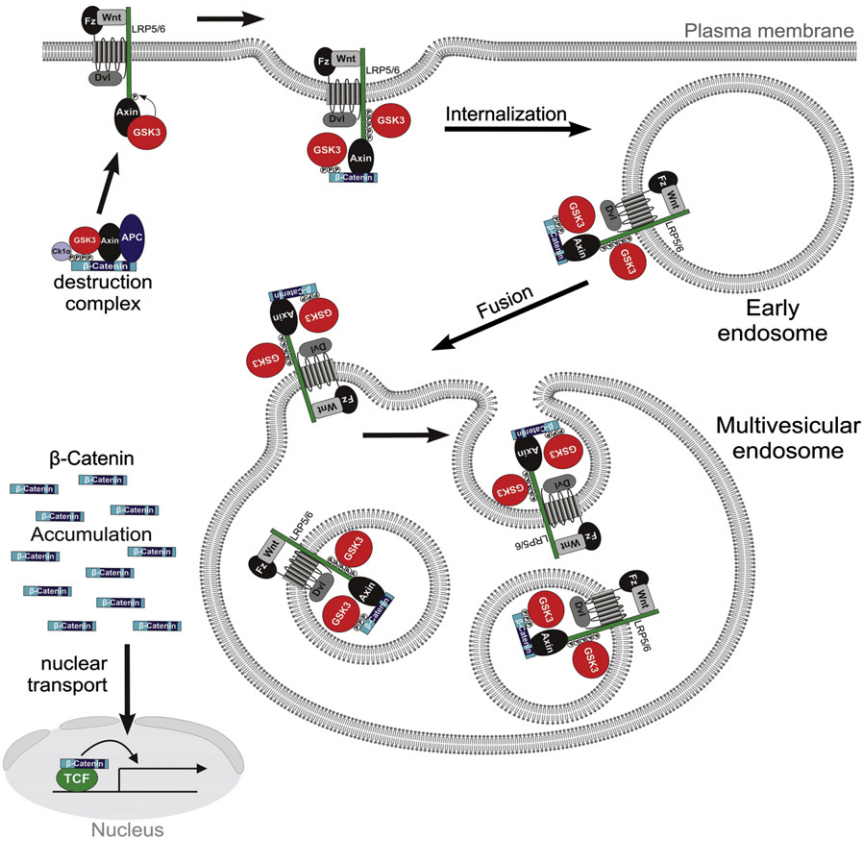

Figure 7. Model of Canonical Wnt Signaling through the Sequestration of GSK3 inside Multivesicular Endosomes

Binding of GSK3 (in red) to the Wnt receptor complex (including phospho-LRP6, phospho-β-Catenin, and other GSK3 substrates such as Dvl, Axin, and APC) sequesters GSK3 inside small intralumenal MVB vesicles, causing its cytosolic substrates such as β-Catenin (in blue) and many other proteins to become stabilized (see text). The initial GSK3 molecules are recruited to the receptor complex bound to Axin, ensuring that the GSK3 fraction bound to the destruction complex is depleted first. Diagram modified from Zeng et al. (2008).

phosphorylated and becomes stabilized, accumulating in the nucleus. Many cellular proteins contain putative GSK3 phosphorylation sites (Table S3) and are also candidates for stabilization by canonical Wnt signaling.

GSK3 Is Relocalized into MVBs upon Wnt Signaling

The results strongly support the GSK3 sequestration hypothesis, providing a solution to the long-standing question of how GSK3 activity is inhibited by Wnt. In coculture experiments, GSK3 accumulated in endosomes containing endocytosed xWnt8-Venus and was depleted from the cytosol. Protease protection studies showed that Wnt3a treatment causes the relocalization of GSK3 inside membrane-bounded organelles. These corresponded to MVBs in cryoimmunoelectron microscopy. Remarkably, Wnt pathway activation by overexpression of CA-LRP6, Dvl, or of Dvl DIX > Ctail construct (Tamai et al., 2004; Capelluto et al., 2002; Metcalfe et al., 2010) relocalized GSK3 into acidic endosomes, decreasing levels of this enzyme in cytosol (Figure 1 and Figure S2). We also observed reductions in cytosolic GSK3 by addition of Wnt3a protein acting on its endogenous receptors (Figures 1A–1C, 1S–1U, Figures 2A–2D, Figures 3B and 3C, Figure 5, and Figure 6; Figures S1A–S1C). Finally, two components of the molecular ESCRT machinery required for the formation of MVBs, HRS and Vps4, were shown to be essential for canonical Wnt signaling in TCF transcriptional reporter and *Xenopus* embryo essays. In epistatic experiments, ESCRT activity was not required for axis induction by Siamois, a transcriptional target downstream of Wnt signaling.

How does this GSK3 sequestration model fit in with the present state of knowledge concerning Wnt signaling? Receptor internalization is required for Wnt to signal (Blitzer and Nusse, 2006; Yamamoto et al., 2006). The proportion of Frizzled receptor destined for degradation versus recycling back to the membrane is regulated by a ubiquitinylation/deubiquitinylation cycle (Mukai et al., 2010), a process that was not investigated here. Bilic et al. (2007) found that aggregates containing Dvl, phosphorylated LRP6, Axin, and GSK3 are induced by Wnt treatment. Designated as LRP6-signalosomes, these aggregates are very prominent in cells in which the Wnt pathway is activated by CA-LRP6, Dvl, or DIX-Ctail overexpression (Bilic et al., 2007, Metcalfe et al., 2010). LRP6-signalosomes were proposed to provide a platform for Wnt signaling on the cytosolic side of early endosomes. The requirement for HRS and Vps4 reported here demonstrates that Wnt signaling requires the formation of multivesicular endosomes (Katzmann et al., 2002; Gruenberg and Stenmark, 2004). There is no contradiction between the LRP6-signalosome model and our results. Sequestration of GSK3 in MVBs is not alone responsible for Wnt signaling. In the early steps of the process, formation of a vesicular platform facing the cytosol recruits the various components to the plasma membrane and early endosomes. In the presence of DN-Dynamin, GSK3-RFP strongly accumulates in the plasma membrane when Wnt signaling is activated (Figure S1F), although Wnt signaling does not take place (Blitzer and Nusse, 2006). Wnt signaling requires the completion of the next step in the endocytic process. Once the neck of the intralumenal vesicles of MVBs is closed, GSK3 will be prevented from equilibrating with the cytosol, explaining why Wnt signaling requires a functional ESCRT machinery.

There is a discrepancy between the requirement of HRS in Wnt signaling described here and studies with HRS mutants in *Drosophila*. Seto and Bellen (2006) reported enhanced

expression of Wg target genes in HRS clones (proposed to be due to decreased lysosomal degradation of Wg), although other authors reported no differences (compared to wild-type tissue) in similar clones (Rives et al., 2006). Perhaps in *Drosophila* some degree of MVB formation is still achieved in the absence of HRS through redundancy in the ESCRT machinery. In the studies presented here, we obtained significant inhibition of canonical Wnt signaling with HRS siRNA, HRS MO, and Vps4-EQ, both in cultured cells and in vivo in *Xenopus*.

Our observations help understand the paradoxical positive and negative effects of GSK3 in early Wnt signaling (Zeng et al., 2008). GSK3 phosphorylation of LRP6 initiates Wnt signaling (MacDonald et al., 2009; Niehrs and Shen, 2010), yet genetic and pharmacological studies show that GSK3 inhibition is sufficient to trigger the canonical Wnt signal (Logan and Nusse, 2004). The sequestration hypothesis helps resolve these apparently contradictory functions, for LRP6 phosphorylation by GSK3 not only initiates signaling but also causes the sequestration of GSK3 from the cytosol.

The key to canonical Wnt signaling is GSK3 inhibition, which results in β-Catenin stabilization (Kimelman and Xu, 2006; Wu and Pan, 2010). Several studies have shown that phosphorylated LRP6 intracellular domain can inhibit GSK3 activity (Mi et al., 2006; Cselenyi et al., 2008; Piao et al., 2008; Wu et al., 2009), although with low affinity (K_i in the 10^{-5} M range). However, GSK3 inhibition has been difficult to demonstrate biochemically. One exception was a study using hypotonic cell lysis, which reported a transient 40% decrease in GSK3 activity that peaked 10 min after Wnt addition (Ding et al., 2000). This early inhibition is likely explained via direct binding of GSK3 to phospho-LRP6. However, this decrease in GSK3 activity disappeared after 1 hr (Ding et al., 2000), whereas stabilized β-Catenin protein continues to accumulate for at least 6 hr after Wnt treatment (Blitzer and Nusse, 2006). We now found that Wnt3a treatment reduced cytosolic GSK3 activity levels by 66% after 4 hr of Wnt3a addition in cells permeabilized with Digitonin (Figure 2A).

Wnt signaling requires the sustained inhibition of GSK3, which is achieved by sequestration inside MVBs. The initial recruitment of the destruction complex (Zeng et al., 2008) would ensure that the GSK3 responsible for β-Catenin degradation is depleted first (explaining in part the insulation from other signaling pathways), followed by other cytosolic GSK3 molecules that bind to additional phosphorylated docking sites provided by GSK3 phosphorylation sites in LRP6, Axin, β-Catenin, Dvl, and APC (Jope and Johnson, 2004; Table S2). Thus, although GSK3 is in stoichiometric excess to Axin, there are many additional potential GSK3 binding sites present in the Wnt receptor-signaling complex (Figure 7). Catalytically inactive DN-GSK3β is not concentrated in MVBs (compare Figures S1G and S1M), suggesting that GSK3 accumulates in MVBs because it binds to its own substrates. Conversely, a GSK3 form that does not bind Axin but is catalytically active can accumulate in LRP6 signalosomes (Figures S1J–S1L), demonstrating that GSK3 molecules not directly associated with the Axin destruction complex can still be sequestered by Wnt signaling. By binding to its own substrates, GSK3 can be depleted from cytosol even when Axin levels are stoichiometrically lower.

Did precedents for a role for the MVB pathway in Wnt signaling exist in the literature? Early on, van den Heuvel et al. (1989) reported that endocytosed Wg accumulates in the MVB matrix in cells responding to the Wg signal in *Drosophila* blastoderm. Acidification by vacuolar/H^+-ATPase is required for canonical Wnt signaling (Cruciat et al., 2010). Dvl overexpression triggers a canonical Wnt signal, and it was reported that this activity correlated with its colocalization with phospholipids in vesicular membranes via its DIX domain (Capelluto et al., 2002). Recently, a fusion protein between the Dvl DIX domain and the Ctail of LRP6 was found to be a very potent activator of Wnt signaling (Metcalfe et al., 2010). Dvl and DIX > Ctail form signalosomes that were initially interpreted as cytoplasmic protein aggregates. However, as shown in Figure S2, the Dvl and DIX > Ctail particles colocalized with FYVE-GFP (a PI3P marker) and also with the acidic dye LysoTracker. These endosomal vesicles depleted GSK3 from the cytoplasm. Their effect was specific because point mutations in the DIX domain (Metcalfe et al., 2010) prevented colocalization with LysoTracker and GSK3. Moreover, inhibiting MVB formation prevented induction of a TCF-Luciferase reporter by the Dvl DIX/LRP6 fusion protein (Figure S2Ba). In conclusion, previous observations were consistent with a role for membrane vesicles in Wnt signaling, but their identity as MVBs that sequester GSK3 was not recognized.

Wnt Is a Regulator of Protein Catabolism

An unexpected finding was that Wnt prolongs the overall rate of cellular protein degradation (Figure 5). The addition of three consecutive GSK3 sites was sufficient to convert GFP into a Wnt-responsive protein (Figure 6). Thus, cytosolic levels of GSK3 are sufficiently depleted by Wnt treatment to stabilize other proteins in addition to β-Catenin. Thus, GSK3 emerges as a protein kinase with a central role in regulating protein catabolism.

Bioinformatic analyses showed that about 20% of the human proteome contains three or more possible primed GSK3 sites, suggesting that many putative Wnt-regulated proteins exist. The principal transcriptional output of Wnt signaling is the interaction between TCF/LEF and β-Catenin (Clevers, 2006). However, many additional transcription factors interact with β-Catenin (reviewed by MacDonald et al., 2009; see their Table S1). It is intriguing that some of the proteins potentially stabilized by Wnt in our list (Table S2) also interact with β-Catenin (e.g., FoxO, HIF1α, Mitf, RAR). Therefore, Wnt signaling may have unforeseen regulatory complexities. Although Wnt signaling can crosstalk with other signal transduction pathways in which GSK3 phosphorylations are involved, such as the BMP/Smad1 pathway (Fuentealba et al., 2007), insulation between pathways is also necessary. The degree of insulation will depend on the relative affinities of the various substrates and their resistance to decreases in levels of free GSK3. In addition crosstalk versus insulation will depend on the type (and activity level) of priming kinase used by the various signaling pathways. The effect of Wnt on overall protein half-life had an absolute requirement for β-Catenin (Figure 5I). This is likely explained by the finding that β-Catenin is required, and its overexpression sufficient, for GSK3 sequestration in MVBs (Figure 4).

Our findings indicate that canonical Wnt provides a signal instructing cells to slow down degradation of many proteins. The recent discovery that LRP6 is phosphorylated at G2/M phase independently of Wnt (Davidson et al., 2009) suggests that the half-life of a multitude of GSK3 target proteins could be under cell cycle control. The list of putative GSK3/Wnt targets identified by our proteomic analyses suggests that Wnt/GSK3 signaling may have wide metabolic effects. In addition it provides a rich resource for discovering possible novel nodes of signaling pathway integration (Table S3).

A Positive Role for Endocytosis in Signal Transduction

Targeting of membrane receptors to MVBs and lysosomes negatively regulates signaling by many growth factor receptors (McKanna et al., 1979; Katzmann et al., 2002). A possible positive role for multivesicular endosomes in the release of Notch intracellular domain to the nucleus has been reported (Coumailleau et al., 2009). In the case of canonical Wnt, the positive role of endosomal trafficking is of a different nature because it is the sequestration of GSK3 in MVBs that generates the signal (Figure 7). This raises the question of whether other plasma membrane receptors might use multivesicular endosomes to sequester proteins bound to their cytoplasmic tails. In this view, specific intracellular proteins could be targeted to MVBs in a growth factor-dependent manner. All eukaryotic cells contain an elaborate ESCRT machinery that generates multivesicular endosomes. Further studies on how the cell biology of endocytic trafficking intersects with signaling by Wnt and other growth factors may have implications for understanding human disease, including cancer.

EXPERIMENTAL PROCEDURES

DNA Constructs and siRNAs

The following GFP or RFP fusion proteins were generated for this study: GSK3-RFP, GSK3-GFP, DN-GSK3-GFP, CA-LRP6-GFP, xDvl-RFP, stabilized mutant β-Catenin-GFP, human HRS-RFP, GFP-GSK3-MAPK reporter, GFP-GSK3mut-MAPK, GFP-GSK3-MAPK-E3mut, and GFP-GSK3-CK1-E3. A pCS2 vector containing amino-terminal Flag-EGFP (GB#U55763) or HA-RFP (GB#AF506027) was used to clone in-frame fusions generated by PCR from ESTs or from constructs generously provided by colleagues listed in the Acknowledgments. The siRNAs targeting human β-Catenin, HRS, and Axin1 were ON-TARGETplus SMARTpool from Thermo Scientific #L-003482, #L-016835, and #L-009625, respectively. The siRNAs used to knock down human GSK3α and GSK3β were Validated Stealth RNAi DuoPak from Invitrogen #45-3210 and #45-1488, respectively.

Immunostaining and Western Blots

For immunostainings, primary antibodies were: anti-GSK3β monoclonal (BD Transduction #610201) at 1:350, and anti-phospho-β-Catenin (Cell Signaling #9561) at 1:350. For cryoimmunoelectron microscopy, antibodies used were chicken IgY anti-GSK3β (Sigma #GW22779) at 1:800 and chicken IgY anti-GFP (Invitrogen #A10262) at 1:250. For western blots, primary antibodies used were the anti-GSK3β monoclonal at 1:1000, anti-β-Catenin (Sigma #C2206) at 1:4000, anti-α-tubulin monoclonal (Calbiochem #CP06) at 1:1500, anti-Flag monoclonal (Sigma #F1804) at 1:1500, and anti-Total-Erk (Cell Signaling #9102) at 1:1000. Secondary antibodies coupled to Infra Red Dyes (IRDye 680 and IRDye 800) at 1:3000 (LI-COR) were used, and western blots were analyzed using a LI-COR Odyssey scanner system.

Statistics

Results are given as the mean ± standard error of the mean (SEM). Statistical analyses were performed with Excel (Microsoft Corp.) applying the two-tailed t test, as appropriate. Differences of means were considered significant at a significance level of 0.05.

Additional Methods

Detailed methods for cell culture, immunostainings, GSK3 enzyme activity measurements, protease protection, cryoimmunoelectron microscopy, *Xenopus* embryo assays, bioinformatic proteomic analyses, and radioactive pulse-chase experiments are provided in Extended Experimental Procedures.

SUPPLEMENTAL INFORMATION

Supplemental Information includes Extended Experimental Procedures, seven figures, and three tables and can be found with this article online at doi:10.1016/j.cell.2010.11.034.

ACKNOWLEDGMENTS

We thank Drs. R. Moon for β-Catenin-GFP and SuperTopFlash reporter, X. He for CA-LRP6, B. van Deurs for dog Rab7-GFP, S. Sokol for Myc-xDvl, M. Bienz for DIX > Ctail-GFP, M. Taira for xWnt8-Venus, P. Woodman for Vps4-EQ-GFP, R. Pagano for Rab5-DsRed-WT, P. De Camilli for DN-Dynamin-GFP, H. Stenmark for FYVE-GFP, H. Clevers for DN-xTcf3, O. Wessely for β-Catenin-DN-xTcf3, P. Lemaire for Siamois, and R. Nusse for Wnt3a-producing L cells. We thank three anonymous referees and members of our laboratories for improving the manuscript, H. Snitkin for her help in processing cultured cells for electron microscopy, U. Lendahl for suggesting the HRS depletion experiments, the Deutsche Forschungsgemeinschaft for supporting R.D. (DO1429/1-1), and the NIH (HD21502-24) for funding. E.M.D.R. is an Investigator of the Howard Hughes Medical Institute.

Received: July 8, 2010
Revised: September 19, 2010
Accepted: October 26, 2010
Published: December 23, 2010

REFERENCES

Angers, S., and Moon, R.T. (2009). Proximal events in Wnt signal transduction. Nat. Rev. Mol. Cell Biol. *10*, 468–477.

Bilic, J., Huang, Y.L., Davidson, G., Zimmermann, T., Cruciat, C.M., Bienz, M., and Niehrs, C. (2007). Wnt induces LRP6 Signalosomes and promotes Dishevelled-dependent LRP6 phosphorylation. Science *316*, 1619–1622.

Bishop, N., and Woodman, P. (2000). ATPase-defective mammalian VPS4 localizes to aberrant endosomes and impairs cholesterol trafficking. Mol. Biol. Cell *11*, 227–239.

Blitzer, J.T., and Nusse, R. (2006). A critical role for endocytosis in Wnt signaling. BMC Cell Biol. *7*, 28.

Bucci, C., Thomsen, P., Nicoziani, P., McCarthy, J., and van Deurs, B. (2000). Rab7: a key to lysosomes biogenesis. Mol. Biol. Cell *11*, 467–480.

Capelluto, D.G., Kutateladze, T.G., Habas, R., Finkielstein, C.V., He, X., and Overduin, M. (2002). The DIX domain targets dishevelled to actin stress fibres and vesicular membranes. Nature *419*, 726–729.

Coumailleau, F., Fürthauer, M., Knoblich, J.A., and González-Gaitán, M. (2009). Directional Delta and Notch trafficking in Sara endosomes during asymmetric cell division. Nature *458*, 1051–1055.

Clevers, H. (2006). Wnt/beta-catenin signaling in development and disease. Cell *127*, 469–480.

Cohen, P., and Frame, S. (2001). The renaissance of GSK3. Nat. Rev. Mol. Cell Biol. *2*, 769–776.

Cruciat, C.M., Ohkawara, B., Acebron, S.P., Karaulanov, E., Reinhard, C., Ingelfinger, D., Boutros, M., and Niehrs, C. (2010). Requirement of prorenin

receptor and vacuolar H^+-ATPase-mediated acidification for Wnt signaling. Science *327*, 459–463.

Cselenyi, C.S., Jernigan, K.K., Tahinci, E., Thorne, C.A., Lee, L.A., and Lee, E. (2008). LRP6 transduces a canonical Wnt signal independently of Axin degradation by inhibiting GSK3's phosphorylation of β-catenin. Proc. Natl. Acad. Sci. USA *105*, 8032–8037.

Davidson, G., Shen, J., Huang, Y.L., Su, Y., Karaulanov, E., Bartscherer, K., Hassler, C., Stannek, P., Boutros, M., and Niehrs, C. (2009). Cell cycle control of Wnt receptor activation. Dev. Cell *17*, 788–799.

Ding, V.W., Chen, R.H., and McCormick, F. (2000). Differential regulation of glycogen synthase kinase 3beta by insulin and Wnt signaling. J. Biol. Chem. *275*, 32475–32481.

Dunn, L.A., and Holz, R.W. (1983). Catecholamine secretion from digitonin-treated adrenal medullary chromaffin cells. J. Biol. Chem. *258*, 4989–4993.

Falguieres, T., Luyet, P., and Gruenberg, J. (2009). Molecular assemblies and membrane domains in multivesicular endosome dynamics. Exp. Cell Res. *315*, 1567–1573.

Fuentealba, L.C., Eivers, E., Ikeda, A., Hurtado, C., Kuroda, H., Pera, E.M., and De Robertis, E.M. (2007). Integrating patterning signals: Wnt/GSK3 regulates the duration of the BMP/Smad1 signal. Cell *131*, 980–993.

Gruenberg, J., and Stenmark, H. (2004). The biogenesis of multivesicular endosomes. Nat. Rev. Mol. Cell Biol. *5*, 317–323.

Jope, R.S., and Johnson, G.V. (2004). The glamour and gloom of glycogen synthase kinase-3. Trends Biochem. Sci. *29*, 95–102.

Katzmann, D.J., Odorizzi, G., and Emr, S.D. (2002). Receptor downregulation and multivesicular-body sorting. Nat. Rev. Mol. Cell Biol. *3*, 893–905.

Kim, N.G., Xu, C., and Gumbiner, B.M. (2009). Identification of targets of the Wnt pathway destruction complex in addition to β-catenin. Proc. Natl. Acad. Sci. USA *106*, 5165–5170.

Kimelman, D., and Xu, W. (2006). β-Catenin destruction complex: insights and questions from a structural perspective. Oncogene *25*, 7482–7491.

Logan, C.Y., and Nusse, R. (2004). The Wnt signaling pathway in development and disease. Annu. Rev. Cell Dev. Biol. *20*, 781–810.

MacDonald, B.T., Tamai, K., and He, X. (2009). Wnt/β-Catenin signaling: components, mechanisms, and diseases. Dev. Cell *17*, 9–26.

McKanna, J.A., Haigler, H.T., and Cohen, S. (1979). Hormone receptor topology and dynamics: Morphological analysis using ferritin-labeled epidermal growth factor. Proc. Natl. Acad. Sci. USA *76*, 5689–5693.

Metcalfe, C., Mendoza-Topaz, C., Mieszczanek, J., and Bienz, M. (2010). Stability elements in the LRP6 cytoplasmic tail confer efficient signalling upon DIX-dependent polymerization. J. Cell Sci. *123*, 1588–1599.

Mi, K., Dolan, P.J., and Johnson, G.V.W. (2006). The low density lipoprotein receptor-related protein 6 interacts with glycogen synthase kinase 3 and attenuates activity. J. Biol. Chem. *281*, 4787–4794.

Mii, Y., and Taira, M. (2009). Secreted Frizzled-related proteins enhance the diffusion of Wnt ligands and expand their signaling range. Development *136*, 4083–4088.

Mukai, A., Yamamoto, M., Awano, W., Watanabe, W., Komada, M., and Goto, S. (2010). Balanced ubiquitylation and deubiquitylation of Frizzled regulate cellular responsiveness to Wg/Wnt. EMBO J. *29*, 2114–2125.

Niehrs, C., and Shen, J. (2010). Regulation of Lrp6 phosphorylation. Cell. Mol. Life Sci. *67*, 2551–2562.

Piao, S., Lee, S.H., Kim, H., Yum, S., Stamos, J.L., Xu, Y., Lee, S.J., Lee, J., Oh, S., Han, J.K., et al. (2008). Direct inhibition of GSK3β by the phosphorylated cytoplasmic domain of LRP6 in Wnt/β-Catenin signaling. PLoS ONE *3*, e4046.

Rives, A.F., Rochlin, K.M., Wehrli, M., Schwartz, S.L., and DiNardo, S. (2006). Endocytic trafficking of Wingless and its receptors, Arrow and DFrizzled-2, in the Drosophila wing. Dev. Biol. *293*, 268–283.

Ryves, W.J., Fryer, L., Dale, T., and Harwood, A.J. (1998). An assay for glycogen synthase kinase 3 (GSK-3) for use in crude cell extracts. Anal. Biochem. *264*, 124–127.

Seto, E.S., and Bellen, H.J. (2006). Internalization is required for proper Wingless signaling in Drosophila melanogaster. J. Cell Biol. *173*, 95–106.

Tamai, K., Zeng, X., Liu, C., Zhang, X., Harada, Y., Chang, Z., and He, X. (2004). A mechanism for Wnt coreceptor activation. Mol. Cell *13*, 149–156.

van den Heuvel, M., Nusse, R., P., Johnston, P., and Lawrence, P.A. (1989). Distribution of the wingless gene product in Drosophila embryos: a protein involved in cell-cell communication. Cell *59*, 739–749.

Vanlandingham, P.A., and Ceresa, B.P. (2009). Rab7 regulates late endocytic trafficking downstream of multivesicular body biogenesis and cargo sequestration. J. Biol. Chem. *284*, 12110–12124.

Wegener, C.S., Malerod, L., Pedersen, N.M., Prodiga, C., Bakke, O., Stenmark, H., and Brech, A. (2010). Ultrastructural characterization of giant endosomes induced by GTPase-deficient Rab5. Histochem. Cell Biol. *133*, 41–55.

Wollert, T., and Hurley, J.H. (2010). Molecular mechanism of multivesicular body biogenesis by ESCRT complexes. Nature *464*, 864–869.

Wu, D., and Pan, W. (2010). GSK3: a multifaceted kinase in Wnt signaling. Trends Biochem. Sci. *35*, 161–168.

Wu, G., Huang, H., Garcia Abreu, J., and He, X. (2009). Inhibition of GSK3 phosphorylation of β-Catenin via phosphorylated PPPSPXS motifs of Wnt coreceptor LRP6. PLoS ONE *4*, e4926.

Yamamoto, H., Komekado, H., and Kikuchi, A. (2006). Caveolin is necessary for Wnt-3a-dependent internalization of LRP6 and accumulation of beta-catenin. Dev. Cell *11*, 213–223.

Zeng, X., Huang, H., Tamai, K., Zhang, X., Harada, Y., Yokota, C., Almeida, K., Wang, J., Doble, B., Woodgett, J., et al. (2008). Initiation of Wnt signaling: control of Wnt coreceptor Lrp6 phosphorylation/activation via frizzled, dishevelled and axin functions. Development *135*, 367–375.

EXTENDED EXPERIMENTAL PROCEDURES

DNA Constructs

All expression constructs made in our laboratory used the pCS2 vector (a gift from Dr. D. Turner) as backbone. GSK3-RFP and GSK3-GFP were cloned behind a PCR product from the EGFP sequence (GB#U55763) or the RFP sequence (GB#AF506027), by inserting in frame a PCR product from *Xenopus laevis* GSK3β (GB#L38492). A Flag tag was also added 5′ to the EGFP sequence. The GSK3-GFP construct was used as template to generate DN-GSK3 by introducing K85R and K86R mutations (He et al., 1995) using the QuickChange II XL kit from Stratagene. The Dsh-RFP constructs was made by exchanging the myc tag for a GFP tag in MycxDvl (gift of S. Sokol). The CA-LRP6-GFP construct was made by cloning the EGFP sequence at the C-terminus end of the CA-LRP6 construct (Tamai et al., 2004). Flag-HDAC4 and flag-JunB constructs were obtained by PCR from ESTs by adding at the N-terminus a Flag tag to the human sequences (GB#BC039904 and GB#BC004250). The human HRS construct (hHRS) was constructed from an EST (GB#BC003565), introducing the RFP sequence at the N-terminus. The stabilized-β-Catenin-GFP construct was made by mutating the GSK3 sites S33A, S37A and T41A (Miller and Moon, 1997) in a wild-type β-Catenin-GFP construct provided by Dr. R. Moon. The Vps4-WT-GFP and Vps4-EQ-GFP constructs (Bishop and Woodman, 2000) were subcloned into the pCS2 plasmid in order to use them for mRNA transcription. A dominant-negative form of the DsRed-Rab5-WT obtained via Addgene (Sharma et al., 2003) was made by introducing a Q79L point mutation (DsRed-Rab5-QL; Wegner et al. [2010]). DN-Dynamin (Addgene plasmid 22197) was from Lee and De Camilli (2002). FYVE-GFP was from Gillooly et al. (2000). The β-Catenin-DN-xTcf3 fusion was made on a pCS2 backbone joining the transactivation domain of *Xenopus* β-Catenin to DN-xTcf3, mimicking an Armadillo-DN-xTcf3 construct initially described by Roose et al. (1998), and was a gift of Dr. O. Wessely. The TCF reporter SuperTopFlash was from Veeman et al. (2003) and was normalized for SV40-Renilla using the Dual-Luciferase Reporter Assay System (Promega #017319). The artificial GFPGSK3-MAPK and GFP-GSK3mut-MAPK constructs were generated by adding to the C terminus of GFP sequences synthetic oligonucleotides encoding for AAASAAASAAASAPASPAAAAAAAAAPPAYDYKDDDDK and AAAAAAAAAAAAAAPASPA AAAAAAAPPAYDYKDDDDK, respectively. The additional constructs used as controls in this study were GFP-GSK3-MAPK-E3mut and GFP-GSK3-CK1-E3. They were generated by addition of the following sequences to the C-terminus of GFP:AAASAAASA AASAPASPAAAAAAAAAAAAADYKDDDDK, or AAASAAASAAASAAASLSGKGNPEEEDVDPPAYDYKDDDDK.

Cell Culture and Transfections

HeLa, 3T3, 293 and L-cells (ATCC #CRL-2648) as well as L-Wnt3a-cells (ATCC #CRL-2647) were cultured in DMEM/10% FBS/Glutamine/Pen/Strep medium. L-cell control conditioned medium and Wnt3a conditioned medium were harvested according to the ATCC protocol (Willert et al., 2003). DNA constructs were transfected with FuGENE 6 (Roche) 24 hr after plating cells. siRNAs were transfected with Lipofectamine 2000 using the reverse transfection protocol (Invitrogen) and analyzed after 48 hr. For RNAi depletion experiments, cells were first transfected with siRNA and, 24 hr later, with DNA. Cycloheximide (Sigma #C-7698) was dissolved in ethanol and used at a final concentration of 20 μg/ml. In the experiments shown in Figure 6, culture medium was supplemented with 4 ng/ml human FGF-2 protein from R&D (#233-FB-025) to promote MAPK/Erk activity.

For each well of 6-well plates, DNAs were transfected in the following amounts: 0.5 μg of Rab7-GFP, GSK3-RFP, GSK3-GFP, Vps4WT-GFP, Vps4EQ-GFP, Flag-HDAC4, Flag-JunB, Dsh-RFP or Axin-GFP; 0.3 μg of GFP-GSK3-MAPK, GFP-GSK3mut-MAPK, GFP-GSK3-MAPK-E3mut or GFP-GSK3-CK1-E3; 0.2 μg of stabilized-β-Catenin-GFP, β-Catenin-GFP, CA-LRP6 and CA-LRP6-GFP; 0.1 μg SuperTopFlash; and 0.01 μg of SV40-Renilla internal control. DNA levels in each well were adjusted by adding empty pCS2 vector, so that each received a total of 1.5 μg of DNA.

Cell Immunostainings

For immunostainings, HeLa, NIH 3T3, and L-cells were grown on two-chamber slides (Lab-Tek II, Fisher Scientific#154461), fixed with fresh 4% paraformaldehyde (Sigma #P6148) for 15 min, and permeabilized by treatment with 0.2% Triton X-100 in DPBS (Gibco) for 10 min. After blocking with 5% goat serum and 0.5% BSA in DPBS for 1 hour (blocking solution), primary antibodies were added overnight at 4°C. Slide chambers were washed 10 min three times with DPBS, and secondary antibodies applied for one hour at room temperature. After three additional washes with DPBS, chambers were removed and slides mounted with Vectashield (Vector #H-1200) containing DAPI stain to visualize DNA. Immunofluorescence was analyzed and photographed using a Zeiss Imager Z.1 microscope with Apotome. For LysoTracker stainings, living cells were exposed to prewarmed medium containing a 1:1000 dilution of LysoTracker Red DND-99 or LysoTracker Blue DND-22 (Invitrogen #L7528 and #L7525, respectively) for 1 min at 37°C, washed with PBS, and fixed with 4% PFA for 15 min at room temperature. Cells were mounted with Vectashield and analyzed as described above.

GSK3 Protection and Kinase Activity Measurements

Protease protection assays were performed essentially as described by Vanlandingham and Ceresa (2009). Control and Wnt-treated confluent L-cells were trypsinized from a 10 cm culture plate and pelleted at 800 rpm in a Sorvall 6000 tabletop centrifuge. Cells were resuspended in buffer (100 mM potassium phosphate pH 6.7, 5 mM $MgCl_2$, 250 mM sucrose) containing 6.5 μg/ml Digitonin and incubated for 5 min at room temperature, followed by 30 min on ice. The Digitonin solution was removed by centrifugation for 5 min at 13,000 rpm in an Eppendorf centrifuge. Permeabilized cells were resuspended in buffer without Digitonin and divided into Eppendorf tubes containing reagents to generate final concentrations of 1 μg/ml Proteinase K (Invitrogen), Proteinase K with

0.1% Triton X-100, or water. After incubation for 10 min at room temperature the reaction was stopped by adding 20 mM PMSF preheated in 5× loading buffer, and heated at 95°C for 10 min before electrophoresis.

For measurements of GSK3 enzymatic activity (Ryves et al., 1998), a similar protocol as for protease protection was used to prepare permeabilized cells. However, a modified buffer was applied (100 mM potassium phosphate pH 6.7, 5 mM $MgCl_2$, 250 mM sucrose, 10 mM DTT, 1 mM PMSF, 1 mM benzamidine, 50 mM NaF, 0.1 μM okadaic acid, 0.5 mM Na3VO4 with or without 0.1% Triton X-100). In total, 12.5 μl of the resuspended permeabilized cells were mixed with 6.25 μl substrate mix (4 mg/ml [phospho-Glycogen Synthase] peptide 2 from Millipore, CA, USA), with or without 200 mM LiCl) and 6.25 μl ATP mix (200 mM Hepes pH 7.5, 50 mM $MgCl_2$, 8 mM DTT, 400 μM ATP, 0.125 μCi [γ32P]ATP, 3,000 Ci/mmol. The mixture was incubated for 8 min at room temperature, and the reaction stopped by spotting 20 μl of the solution onto P81 ion-exchange paper (Whatman), dried and washed three times in 100 mM phosphoric acid for 5 min (Ryves et al., 1998). The radioactivity of each sample was determined by scintillation counting and corrected for total protein content.

Cryoimmunoelectron Microscopy

For cryoimmunoelectron microscopy, 3T3 fibroblasts were treated with or without Wnt3a conditioned medium for 6 hr. HeLa cells expressing GSK3-GFP with or without CA-LRP6 were fixed 12 hr after transfection. Confluent 10 cm dishes were incubated with 3 ml of serum-free medium containing cryo-EM fixative (final concentrations: 4% paraformaldehyde, 0.2 M PHEM buffer (120 mM Pipes, 50 mM Hepes, 20 mM EGTA, 4 mM $MgCl_2$ pH 7.0), and 0.4% glutaraldehyde) for 1 hr. This solution was replaced by one containing the same fixatives diluted in 0.1 M PHEM buffer and incubated for 90 min. Cells were collected using a Teflon scraper, divided into several Eppendorf tubes, and centrifuged for 10 min at 10,000 rpm. The pellets were carefully washed three times for 10 min with 0.1 M PHEM buffer. The specimens were then subjected to cryo sectioning and labeling and immunoelectron microscopy using chicken IgY anti-GSK3β (Sigma #GW22779) or chicken IgY anti-GFP (Invitrogen #A10262) followed by 15 nm Protein A-Gold, as described (Guo et al., 2009; Slot and Geuze, 2007; Liou et al., 1996).

Xenopus Embryo Assays

For *Xenopus* embryo microinjection, DNAs were linearized with NotI and mRNAs synthesized with mMessage mMachine SP6 (Ambion). For embryo secondary axis induction, 80 pg of *CALRP6* mRNA or 80 pg *β-Catenin*-Myc mRNA (Yost et al., 1998) were injected into a ventral vegetal cell at 8-cell stage. The antisense oligo Morpholino (MO) against *Xenopus laevis* HRS had the following sequence: TGCCGCTTCCTCTTCCCATTGCGAA. This MO targets both the *Xenopus laevis* sequence and that of *X. tropicalis*. Four nl of 0.3 mM Morpholino were coinjected with *CA-LRP6* or *β-Catenin* mRNA, with or without 10 pg of mRNA coding for human *HRS*. For *Vps4-WT* or *Vps4-EQ*, 500 pg of mRNA were coinjected. For *Siamois* mRNA (Lemaire et al., 1995), 20 pg were injected once ventrally. In situ hybridizations of injected embryos were carried out at stage 19. Embryos receiving a single ventral injection of HRS MO or Vps4-EQ mRNA do not survive past stage 23. The effects of Vps4-EQ or HRS-MO on endogenous axis development could not be ascertained as their injection into the entire embryo disrupts gastrulation. Staining of embryos injected with LacZ mRNA was performed as described (Reversade and De Robertis, 2005).

Ectodermal explants harvested for western blot (Figure S6D) were injected four times with 100 pg *Flag-HDAC* mRNA with or without 50 pg *xWnt8* mRNA. Animal caps were cut at stage 9, cultured until stage 10.5, and homogenized in lysis buffer (50 mM Tris pH 7.4, 150 mM NaCl, 1 mM EDTA, 1% Triton X-100, and Protease inhibitor #10863600 from Roche). Ectodermal explants harvested for Luciferase gene reporter assay (Figure 3F) were injected four times with 50 pg of SuperTopFlash DNA and 80 pg *CA-LRP6* mRNA, with or without HRS MO.

In Silico Identification of Putative GSK3 Phosphorylation Sites

To identify putative human GSK3 protein targets, a copy of the complete human proteome was downloaded from the Ensembl website (http://www.ensembl.org, release 55) (Hubbard, 2009). A custom Perl algorithm was used to generate a list of all human proteins containing at least 2 consecutive GSK3 sites (consensus: S/TXXXS/T[PO3]) primed by any Serine or Threonine (Puntervoll et al., 2003). To estimate the potential physiological relevance of the phosphorylation site predictions, we examined the evolutionary conservation of each of the motifs identified. Proteins in the list were grouped by gene family as defined by Ensembl. For each family, an alignment of family members belonging to the following species was retrieved from the Ensembl database: human, mouse, opossum, platypus, chicken, *Xenopus tropicalis*, zebrafish, pufferfish (*Tetraodon nigroviridis*), ascidian (*Ciona intestinalis*), nematode (*C. elegans*), and fruit fly (*D. melanogaster*). Putative phosphorylation motifs were subsequently identified in these sequences by the same bioinformatic method as above, and their conservation assayed by counting the number of genes containing a motif at the same position in the alignment (designated Conservation Index). A complete list of predicted GSK3 phosphorylation targets in the human proteome and their evolutionary conservation is provided in Table S3.

Radioactive ^{35}S Methionine Pulse-Chase Experiments

HEK293T cells at 70%-80% confluence were starved for Methionine with DMEM culture medium lacking this amino acid supplemented with 10% dialyzed serum (Invitrogen, NY, USA) for 30 min. Cells were metabolically labeled with 0.2 mCi/ml 35S-Methionine (Perkin Elmer, MA, USA) for 30 min. Culture medium was replaced by nonradioactive conditioned medium (supplemented with an additional 15 mg/l Methionine, final concentration 45 mg/l) from control L-cells or L-Wnt3a-cells (or Wnt3a purified protein, Willert

et al., 2003). Cells were harvested at different chase time intervals in standard lysis buffer (50 mM Tris, 150 mM NaCl, 1 mM EDTA, 1% Triton X-100 pH 7.4, plus Roche protease inhibitor cocktail) and spotted on a Whatman 3MM paper preblocked with 0.1% Methionine, or analyzed by SDS-PAGE. Dry paper pieces containing the spotted samples were placed in 10% cold Trichloroacetic acid (TCA) for 20 min and transferred into a boiling solution of 5% TCA for 15 min to hydrolyze radioactive charged Met-tRNA. Paper fragments were then washed again with 5% TCA and 95% ethanol at room temperature and dried. The radioactivity of each sample was determined by scintillation counting and normalized for total protein content (measured by the BCA kit from Pierce). Protein half-life values were calculated using the polynomial regression method using MS Excel. The half-life of control and Wnt-stimulated cells was calculated from the slope of the regression function as the mean from four pulse-chase experiments. Protein gels from samples chased for 6 hr were dried using the DryEase Mini-Gel drying system (Invitrogen, NY, USA) and used for autoradiography. The GSK3 inhibitor BIO (Meijer et al., 2003) was used at 5 μM.

SUPPLEMENTAL REFERENCES

Boyle, W.J., Smeal, T., Defize, L.H., Angel, P., Woodgett, J.R., Karin, M., and Hunter, T. (1991). Activation of protein kinase C decreases phosphorylation of c-Jun at sites that negatively regulate its DNA-binding activity. Cell *64*, 573–584.

Embi, N., Rylatt, D.B., and Cohen, P. (1980). Glycogen synthase kinase-3 from rabbit skeletal muscle. Separation from cyclic-AMP-dependent protein kinase and phosphorylase kinase. Eur. J. Biochem. *107*, 519–527.

Ferkey, D.M., and Kimelman, D. (2002). Glycogen synthase kinase 3b mutagenesis identifies a common binding for GBP and Axin. J. Biol. Chem. *277*, 16147–16152.

Gillooly, D.J., Morrow, I.C., Lindsay, M., Gould, R., Bryant, N.J., Gaullier, J.M., Parton, R.G., and Stenmark, H. (2000). Localization of phosphatidylinositol 3-phosphate in yeast and mammalian cells. EMBO J. *19*, 4577–4588.

Guo, X., Tu, L., Gumper, I., Plesken, H., Novak, E.K., Chintala, S., Swank, R.T., Pastores, G., Torres, P., Izumi, T., et al. (2009). Involvement of Vps33a in the fusion of uroplakin-degrading multivesicular bodies with lysosomes. Traffic *10*, 1350–1361.

He, X., Saint-Jeannet, P., Woodgett, J.R., Varmus, H.E., and Dawid, I.B. (1995). Glycogen synthase kinase-3 and dorsoventral patterning in Xenopus embryos. Nature *374*, 617–622.

Hubbard, T.J., Aken, B.L., Ayling, S., Ballester, B., Beal, K., Bragin, E., Brent, S., Chen, Y., Clapham, P., Clarke, L., et al. (2009). Ensembl 2009. Nucleic Acids Res. *37*, D690–D697.

Jia, J., Amanai, K., Wang, G., Tang, J., Wang, B., and Jiang, J. (2002). Shaggy/GSK3 antagonizes Hedgehog signalling by regulating Cubitus interruptus. Nature *416*, 548–552.

Lee, E., and De Camilli, P. (2002). Dynamin at actin tails. Proc. Natl. Acad. Sci. USA *99*, 161–166.

Lemaire, P., Garrett, N., and Gurdon, J.B. (1995). Expression cloning of Siamois, a Xenopus homeobox gene expressed in dorsal-vegetal cells of blastulae and able to induce a complete secondary axis. Cell *81*, 85–94.

Liou, W., Geuze, H.J., and Slot, J.W. (1996). Improving structural integrity of cryosections for immunogold labeling. Histochem. Cell Biol. *106*, 41–58.

Meijer, L., Skaltsounis, A.L., Magiatis, P., Polychronopoulos, P., Knochaert, M., Leost, M., Ryan, X.P., Vonica, C.A., Brivanlou, A., Dajani, R., et al. (2003). GSK-3-selective inhibitors derived from Tyrian purple indirubins. Chem. Biol. *10*, 1255–1266.

Miller, J.R., and Moon, R.T. (1997). Analysis of the signaling activities of localization mutants of beta-catenin during axis specification in Xenopus. J. Cell Biol. *139*, 229–244.

Puntervoll, P., Linding, R., Gemünd, C., Chabanis-Davidson, S., Mattingsdal, M., Cameron, S., Martin, D.M., Ausiello, G., Brannetti, B., Costantini, A., et al. (2003). ELM server: a new resource for investigating short functional sites in modular eukaryotic proteins. Nucleic Acids Res. *31*, 3625–3630.

Reversade, B., and De Robertis, E.M. (2005). Regulation of ADMP and BMP2/4/7 at opposite embryonic poles generates a self-regulating morphogenetic field. Cell *123*, 1147–1160.

Rocques, N., Abou Zeid, N., Sii-Felice, K., Lecoin, L., Felder-Schmittbuhl, M.P., Eychène, A., and Pouponnot, C. (2007). GSK-3-mediated phosphorylation enhances Maf-transforming activity. Mol. Cell *28*, 584–597.

Roose, J., Molenaar, M., Peterson, J., Hurenkamp, J., Brantjes, H., Moerer, P., van de Wetering, M., Destrée, O., and Clevers, H. (1998). The Xenopus Wnt effector XTcf-3 interacts with Groucho-related transcriptional repressors. Nature *395*, 608–612.

Sharma, D.K., Choudhury, A., Singh, R.D., Wheatley, C.L., Marks, D.L., and Pagano, R.E. (2003). Glycosphingolipids internalized via caveolar-related endocytosis rapidly merge with the clathrin pathway in early endosomes and form microdomains for recycling. J. Biol. Chem. *278*, 7564–7572.

Singh, S.B., Tandon, R., Krishnamurthy, G., Vikram, R., Sharma, N., Basu, S.K., and Mukhopadhyay, A. (2003). Rab5-mediated endosome-endosome fusion regulates hemoglobin endocytosis in Leishmania donovani. EMBO J. *22*, 5712–5722.

Slot, J.W., and Geuze, H.J. (2007). Cryosectioning and immunolabeling. Nat. Protoc. *10*, 2480–2491.

Veeman, M.T., Slusarski, D.C., Kaykas, A., Louie, S.H., and Moon, R.T. (2003). Zebrafish prickle, a modulator of noncanonical Wnt/Fz signaling, regulates gastrulation movements. Curr. Biol. *13*, 680–685.

Willert, K., Brown, J.D., Danenberg, E., Duncan, A.W., Weissman, I.L., Reya, T., Yates, J.R., and Nusse, R. (2003). Wnt proteins are lipid-modified and can act as stem cell growth factors. Nature *423*, 448–452.

Yost, C., Farr, G.H., Pierce, S.B., Ferkey, D.M., Chen, M.M., and Kimelman, D. (1998). GBP, an inhibitor of GSK-3 is implicated in Xenopus development and oncogenesis. Cell *93*, 1031–1041.

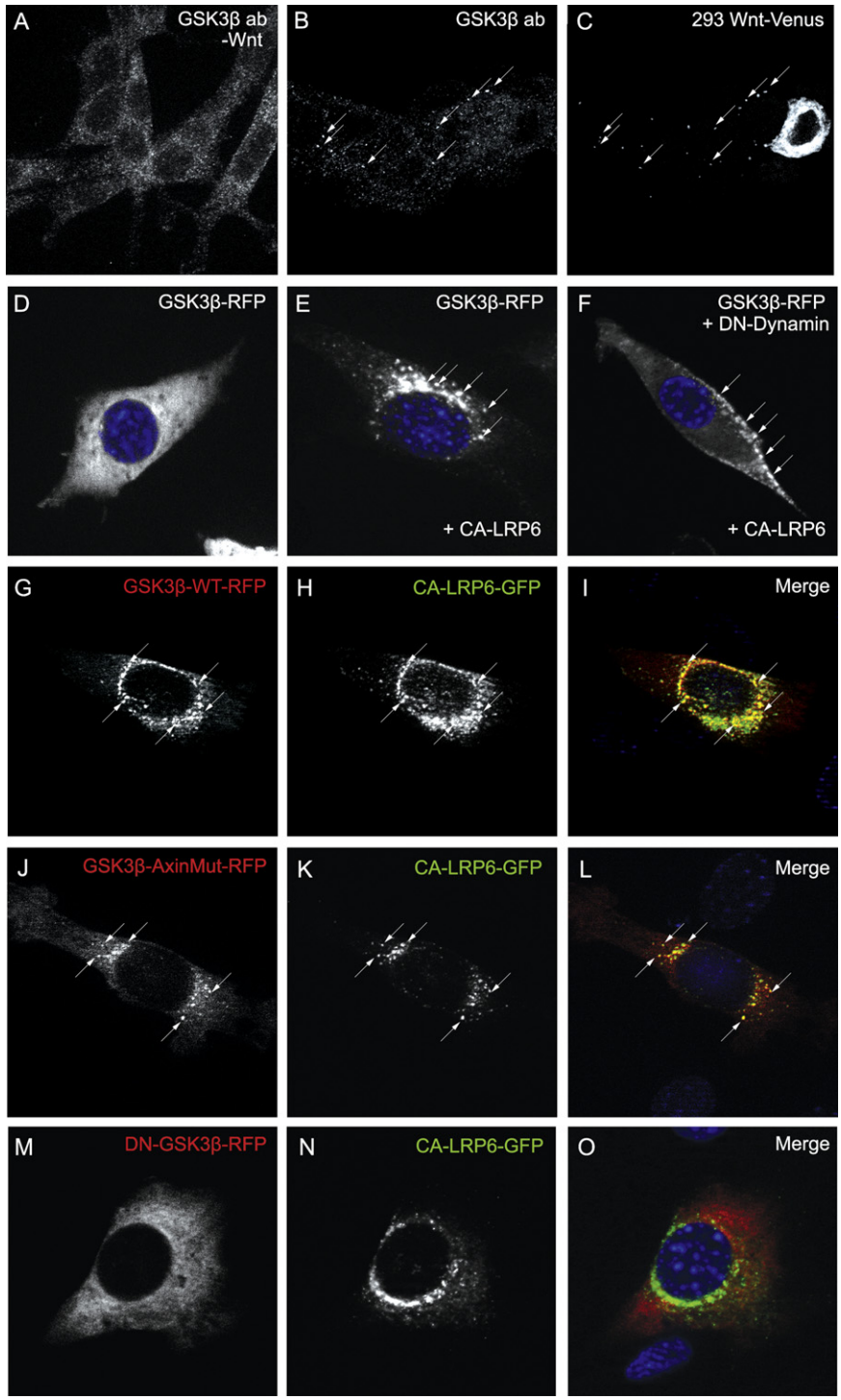

Figure S1. Wnt8-Venus or CA-LRP6 Sequester GSK3 in Dynamin-Dependent Signalosomes; GSK3 Mutated in Its Axin-Binding Site Can Accumulate in MVBs, but Catalytically Inactive DN-GSK3 Does not, Related to Figure 1

(A) Control 3T3 cells (minus Wnt) stained with an anti-GSK3β antibody.

(B) Coculture with 293T secreting Wnt8-Venus caused the relocalization of endogenous GSK3β in 3T3 cells that endocytosed Wnt. Arrows indicate Wnt8-Venus endosomes that sequestered endogenous GSK3β. Cytosolic levels of GSK3β were decreased with respect to control 3T3 cells minus Wnt, but the depletion was less compelling than that observed with GSK3-RFP in Figures 1A–1F.

(C) A 293T cell strongly secreting Wnt8-Venus surrounded by 3T3 cells endocytosing the protein (arrows). Note that Wnt-Venus and GSK3β overlap in endosomes.

(D–F) The GSK3 relocalization caused by CA-LRP6 is Dynamin-dependent. The homogenous cytoplasmic localization of GSK3-RFP became vesicular and concentrated close to the nucleus upon CA-LRP6 transfection. When cotransfected with DN-Dynamin, GSK3-RFP translocated to the membrane instead, and could not be further internalized into intracellular LRP6 signalosomes (arrows).

(G–I) Wild-type GSK3-RFP colocalized with CA-LRP6-GFP signalosomes in 3T3 cells.

(J–L) GSK3-RFP mutated so that its Axin-binding site was inactivated, GSK3-F291L (Ferkey and Kimelman, 2002), was still sequestered from the cytoplasm by CA-LRP6-signalosomes (arrows). Colocalization was reduced in comparison to wild-type GSK3-RFP. This result indicates that binding of GSK3 to Axin is not essential for its localization within Wnt signaling endosomes.

(M–O) Catalytically inactive DN-GSK3-RFP does not associate with CA-LRP6-GFP. This suggests that only active GSK3 molecules associate with CA-LRP6-induced MVBs via binding to its own substrates. To ensure a proper phosphorylation of CA-LRP6 by endogenous GSK3 and its subsequent internalization, DN-GSK3-RFP was transfected in relatively low concentrations in this experiment.

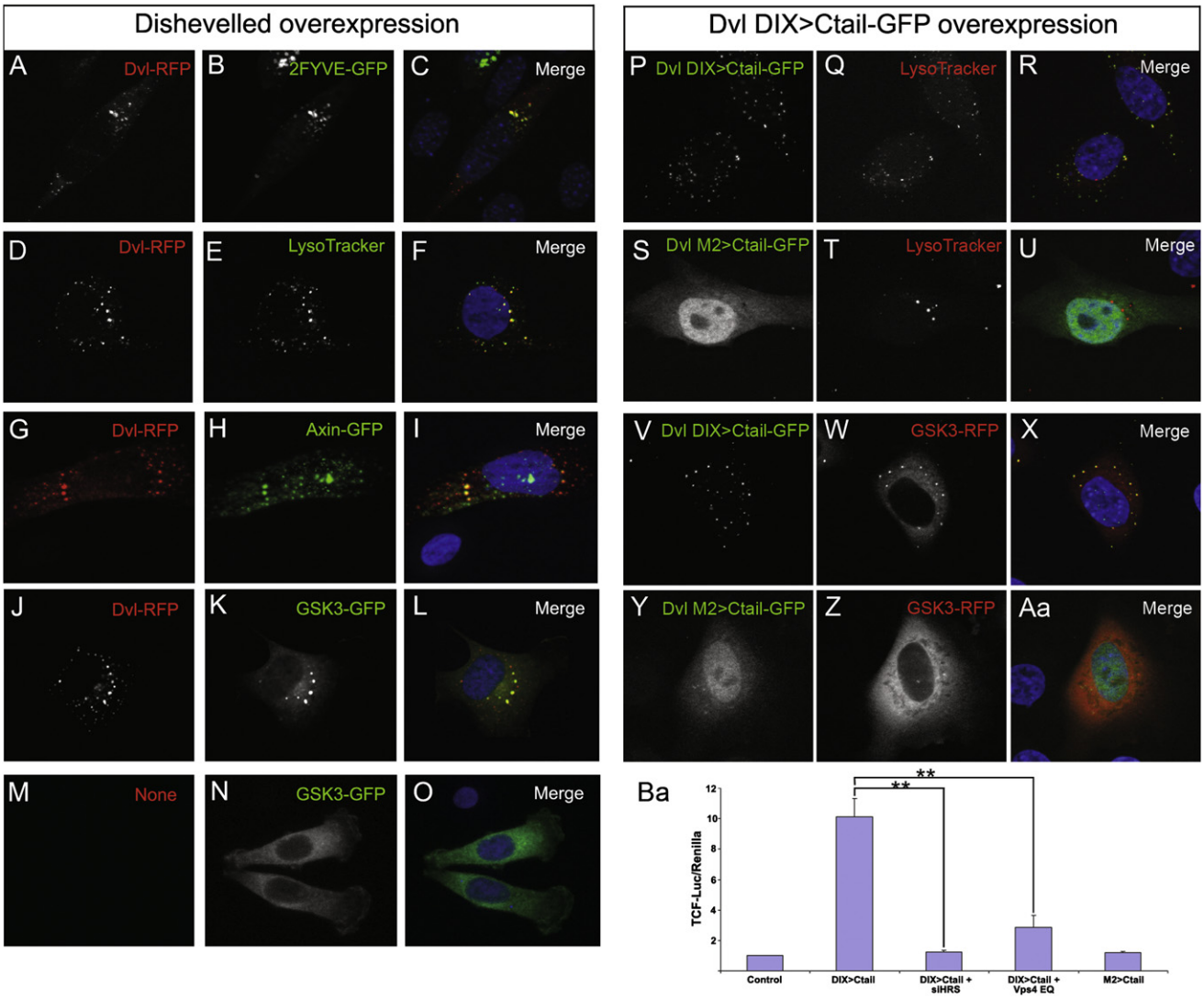

Figure S2. Overexpressed Dishevelled or Dvl DIX>Ctail-GFP Colocalized with GSK3 in Acidic Endosomal Vesicles in HeLa Cells, Related to Figure 1

Panels A to O, on the left side, show analyses of Dvl-RFP in cultured cells, Panels P to Ba, on the right side, show experiments with the Dvl DIX>Ctail reagent of Marianne Bienz.

(A–C) Dvl-RFP puncta colocalize with FYVE-GFP, a reagent that specifically recognizes PI3P, a key component of endosomes (Gillooly et al., 2000). This is important because Dvl was previously thought to form cytoplasmic "protein aggregates" rather than being located in endosomes.

(D–F) Dvl-RFP particles concentrate LysoTracker dye and therefore correspond to acidic endosomes such as MVBs or lysosomes.

(G–I) Dvl-RFP colocalizes with Axin, an essential component of LRP6-signalosomes.

(J–L) Dvl-RFP (red) caused GSK3-GFP (green) to translocate into vesicle-like particles. These results show that Dvl overexpression is sufficient to partially sequester GSK3-RFP in acidic signalosomes.

(M–O) In the absence of transfected Dvl, GSK3 was distributed uniformly throughout the cytosol in these two HeLa cells lacking Dvl-RFP. Note that the cytosolic levels of GSK3-RFP were higher that in Dvl overexpressing cells.

(P–U) Dvl DIX>Ctail-GFP signalosomes, but not the control inactive point mutation M2>Ctail-GFP (Metcalfe et al., 2010), colocalized with LysoTracker dye. This demonstrates that Dvl DIX>Ctail signalosomes are acidic organelles, rather than protein aggregates.

(V–Aa) Dvl DIX>Ctail-GFP signalosomes, but not the inactive M2>Ctail-GFP control, colocalize with GSK3-RFP. Note that the cytosolic levels of GSK3-RFP are significantly reduced when DIX>Ctail sequesters GSK3 (compare panels W and Z).

(Ba) Canonical Wnt signaling by the Dvl DIX>Ctail fusion protein is inhibited by HRS siRNA or by expression of dominant-negative Vps4-EQ (brackets). The M2>Ctail point mutation which does not localize to acidic vesicles did not induce a Wnt signal. Human 293T cells were transfected with TCF-Luciferase and SV40 promoter-Renilla, and activity levels measured 12 hr later. This experiment shows that signaling by the DIX>Ctail construct requires components of the ESCRT-0 and ESCRT-III machinery.

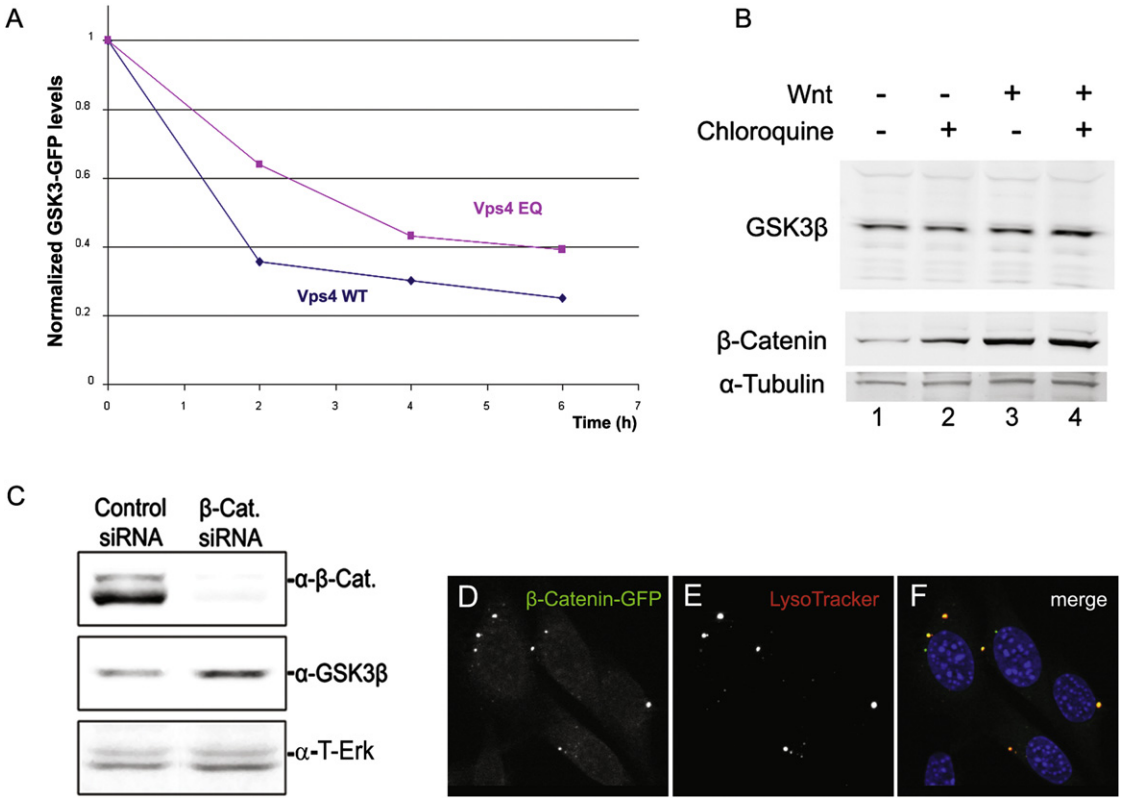

Figure S3. GSK3-GFP Is Partially Stabilized when Multivesicular Endosome Function Is Inhibited; β-Catenin Depletion Was Effective and Caused a Modest Increase in Endogenous GSK3 Levels, Related to Figure 3

(A) In this experiment we asked whether the ESCRT multivesicular endosome machinery is required for the degradation of GSK3. The results presented here suggest that GSK3 is degraded, but only in part, through the endosomal pathway. 293T cells were transfected with GSK3-GFP construct and with Vps4-WT or Vps4-EQ construct. Cells were treated the next day with 20 μg/ml of Cycloheximide, protein extracts harvested at different time points, and analyzed by western blot. Levels of GSK3-GFP were normalized using anti-total-Erk antibody as loading control. Vps4 is an essential component of the ESCRT-III machinery. The graph shows increased stabilization of GSK3-GFP when Vps4-EQ, a dominant-negative form of the protein, is cotransfected. This indicates that GSK3 is degraded in part through the lysosomal pathway. However, total endogenous GSK3 levels do not change much during Wnt3a signaling (Figure 3B; Blitzer and Nusse, 2006). The intensity of the Wnt signal may depend on the period of time that GSK3 remains sequestered in MVBs.

(B) Treatment with Chloroquine, a lysosomal inhibitor, stabilizes GSK3 during Wnt signaling. Levels of endogenous GSK3β did not significantly change when 293T cells were treated with Chloroquine or Wnt3a conditioned medium (lanes 2 or 3, respectively), but increased when simultaneously treated with Wnt3a and Chloroquine (compare lanes 1 and 4). Note that β-Catenin levels also slightly increase with Chloroquine treatment. This result indicates that GSK3 is degraded in part in the lysosomal compartment, particularly during Wnt signaling.

(C) β-Catenin is efficiently depleted by siRNA. We noticed that GSK3β was stabilized by about 40% (by densitometry of western blots) after 2 days of β-Catenin depletion. β-Catenin is required for the formation of Wnt MVBs. T-Erk antibody was used as loading control.

(D–F) Overexpression of wild-type β-Catenin-GFP induces cytoplasmic vesicle-like structures that concentrate LysoTracker (72% ± 9% colocalization of LysoTracker and β-Catenin-GFP in transfected cells, n = 75).

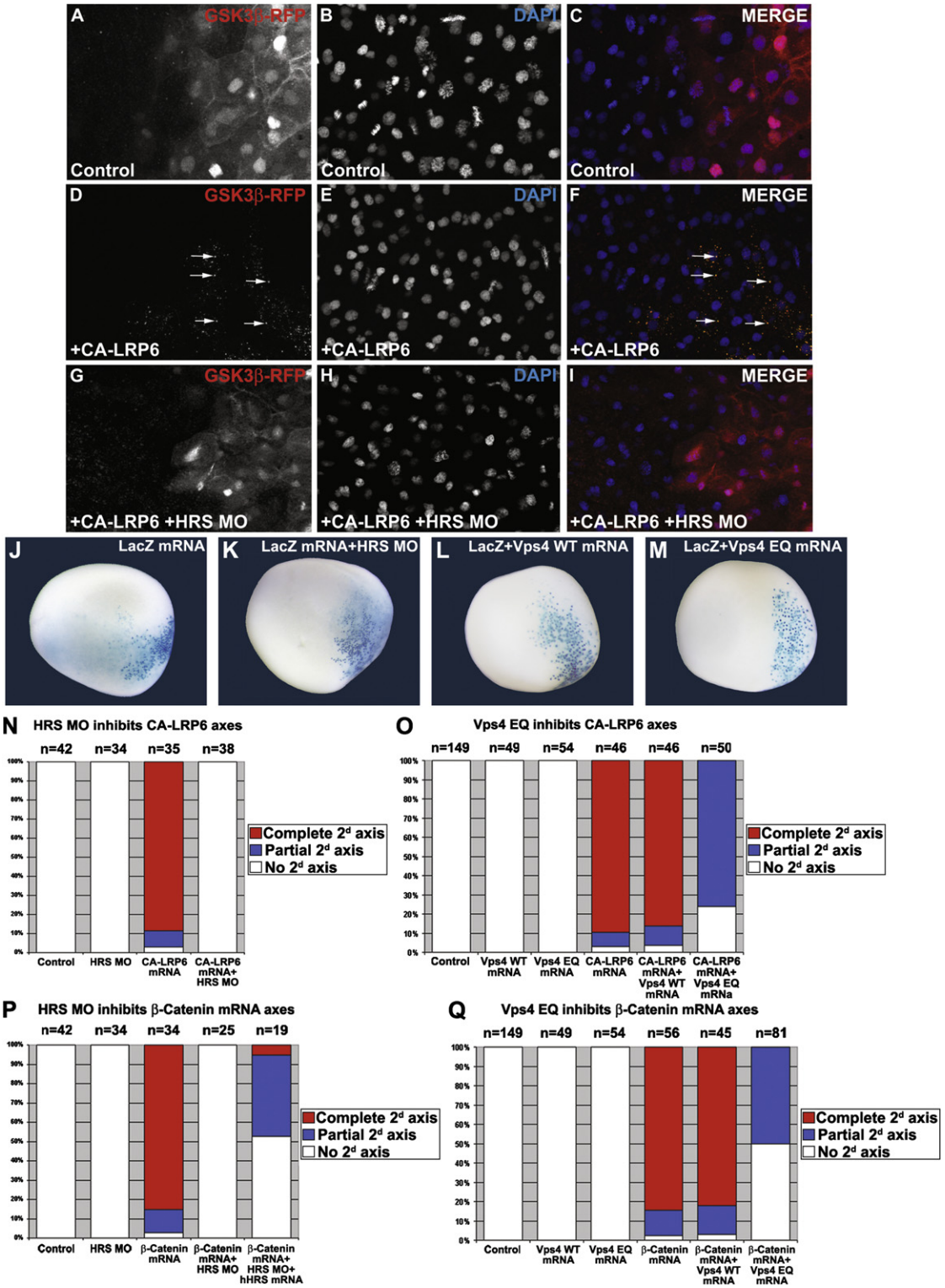

Figure S4. HRS Is Required for the Relocalization of GSK3-RFP into Particles Induced by CA-LRP6, and HRS and Vps4 Are Required for Secondary Axis Induction by CA-LRP6 or β-Catenin mRNA in *Xenopus*, Related to Figure 3

(A–C) *Xenopus* embryos animal explants (at stage 9) previously injected with GSK3-RFP mRNA in one cell show a homogenous localization of GSK3 (in red) in the injected progeny.

(D–F) When coinjected with CA-LRP6 mRNA, GSK3-RFP relocalizes into small puncta (arrows).

(G–I) Coinjection of HRS MO with GSK3-RFP and CA-LRP6 mRNAs abolishes the relocalization of GSK3 induced by CA-LRP6. Note that there are no signs of cell death or changes in the number of mitotic figures when HRS MO is injected.
(J–M) Embryos coinjected with nuclear *LacZ* mRNA (100 pg) and HRS MO, Vps4 EQ mRNA or Vps4 WT mRNA. The embryos show clear nuclear staining of the lacZ, indicating that the injected cells are dividing and healthy at this stage of development (neurula stage 15).
(N) Coinjection of HRS MO blocked the formation of secondary axes induced by a single ventral injection of CA-LRP6 mRNA (quantification of embryos shown in Figures 3G–3I).
(O) Coinjection of CA-LRP6 and Vps4-WT mRNAs showed no difference in the frequency of secondary axes induced by CA-LRP6 mRNA alone. In contrast, co-injection of CA-LRP6 mRNA and Vps4-EQ mRNA, a dominant-negative form of this ESCRT-III complex protein, inhibited the formation of complete secondary axes; only partial induced secondary axes remained (quantification for Figures 3R–3T).
(P) Coinjection of HRS MO blocked the formation of secondary axes induced by β-Catenin mRNA. Importantly, axis formation was partially rescued by coinjection of mRNA coding for human HRS (hHRS), illustrating that the HRS MO designed for this study is specific (quantification for Figures 4M–4O).
(Q) Coinjection of *β-Catenin* and Vps4-EQ mRNAs, but not Vps4-WT mRNA, inhibited formation of complete secondary axes, with only partial secondary axes remaining (quantification for Figures 4P–4R).

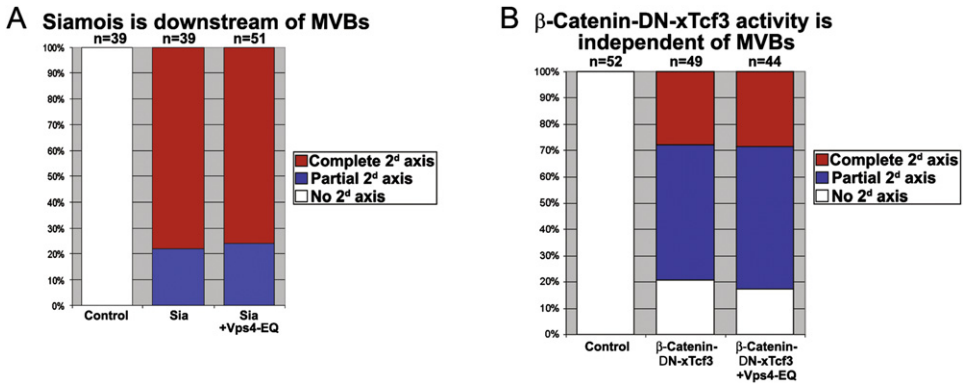

Figure S5. The Downstream Target of Wnt Signaling Siamois, or a Fusion Protein between β-Catenin and Tcf3, Are Not Affected by Inhibiting MVB formation with Vps4-EQ, Related to Figure 4

(A) Histogram showing the number of complete and partial secondary axes obtained in two independent experiments. No difference was observed when Vps4-EQ mRNA (500 pg) was coinjected with *Siamois* mRNA (20 pg) (Lemaire et al., 1995). In parallel experiments, HRS MO was unable to block secondary axes induced by *Siamois* mRNA, even though HRS MO was very effective when coinjected with CA-LRP6 mRNA (data not shown). However, the combination of *Siamois* mRNA and HRS MO tended to cause exogastrulation in embryos.

(B) Histogram showing the number of complete and partial secondary axes obtained in three independent experiments. No difference was observed when Vps4-EQ mRNA was coinjected with β-Catenin-DN-xTcf3 mRNA (125 pg).

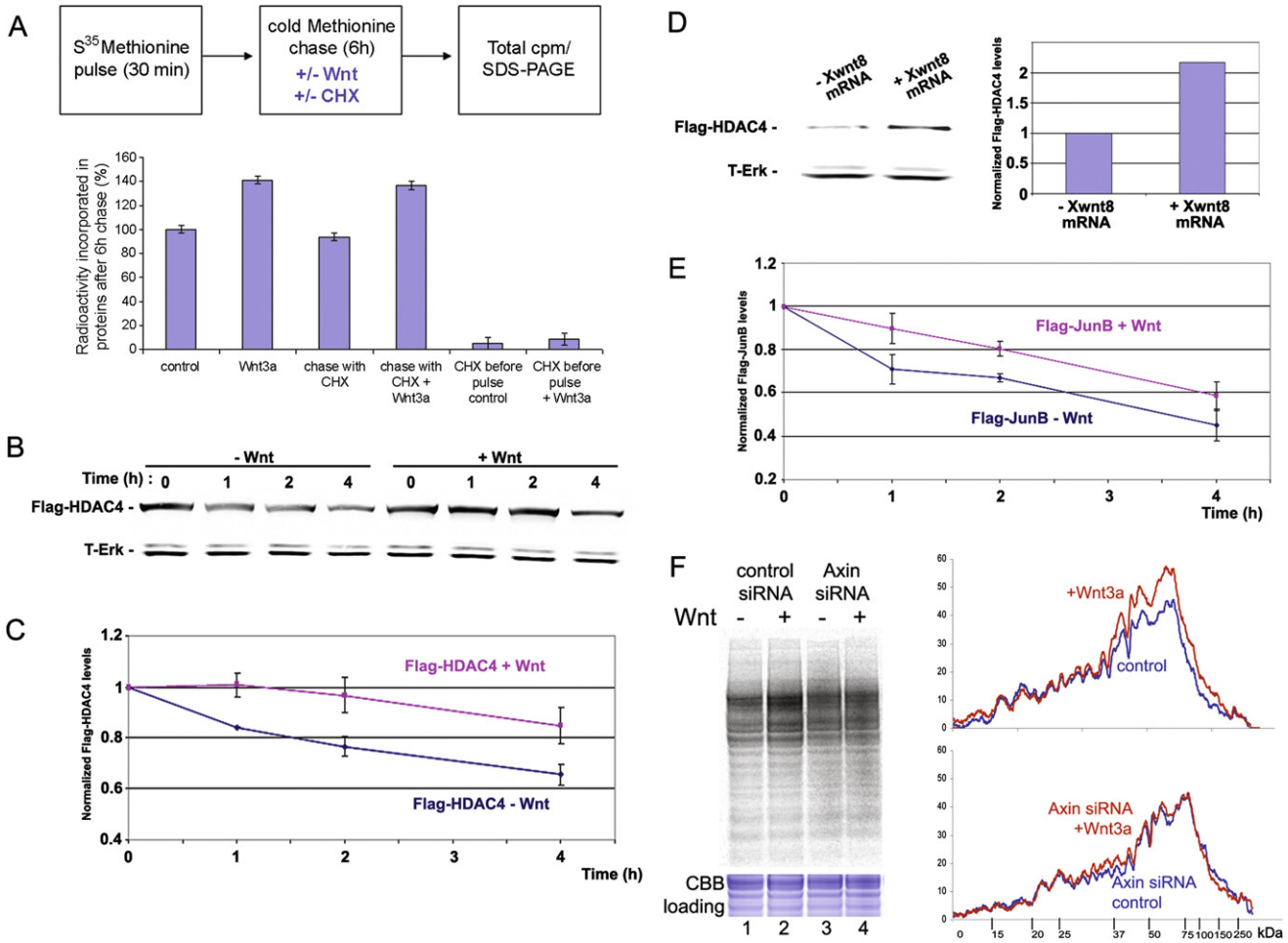

Figure S6. Cycloheximide Chase Experiments Showing that Total Proteins, HDAC4, and JunB Are Stabilized by Wnt, and that Axin Is Required for the Increase of Protein Half-Life Triggered by Wnt, Related to Figure 5

(A) 293T cells were labeled with S35 methionine for 30 min and chased with an excess of cold (unlabeled) Methionine for 6 hr with or without Wnt3a and Cycloheximide (CHX). Proteins from cells treated with Wnt3a conditioned medium were 45% more stable than conditioned medium controls after 6 hr of cold chase. The addition of Cycloheximide, an inhibitor of protein synthesis, did not affect this Wnt-mediated effect, showing that a direct post-translational, Wnt target gene independent, mechanism causes protein stabilization by Wnt3a. (In addition, note that stabilization cannot be due to translational regulation by microRNA, because S35 Met incorporation is completed before Wnt is added.) The last two samples, in which CHX was added before labeling, serve as controls to show that the CHX treatment was effective.

(B) 293T cells were transfected with a Flag-HDAC4 construct and treated the following day with 20 μg/ml of Cycloheximide with control or Wnt3a conditioned medium. Proteins were extracted at different time points and analyzed by western blot using an anti-Flag antibody; anti-total-Erk was used as loading control. The cells treated with Wnt showed slower degradation of Flag-HDAC4 protein.

(C) Quantification of the western blot above by LI-COR Odyssey Imager, confirming the stabilization of Flag-HDAC4 by Wnt. Levels of Flag-HDAC4 were normalized using anti-total-Erk antibody as loading control. An experiment using a Flag-HDAC4 construct mutated in the GSK3 sites showed little difference between the protein levels in presence or absence of Wnt, indicating that the three GSK3 sites in HDAC4 are required to render the protein sensitive to Wnt signaling (data not shown).

(D) *Xenopus* 4 or 8-cell embryos were injected into the animal pole four times with 100 pg of *HDAC4-Flag* mRNA with or without 50 pg of *Xwnt8* mRNA, animal explants prepared at blastula, and homogenized at stage 10. The western blot shows increased levels of HDAC4-Flag protein in presence of xWnt8. Its quantification (using the LI-COR Odyssey scanner system) revealed a 2.2 fold increased level of HDAC4-Flag protein in the presence of xWnt8.

(E) Cycloheximide chase experiment showing that a Flag-JunB construct is stabilized upon Wnt treatment. JunB contains only two GSK3 sites (Table S2). Other proteins with only two GSK3 sites might be regulated by Wnt.

(F) Radioactive pulse-chase experiment after 6 hr of chase showing that the Wnt-regulated prolongation of protein half-life is abolished when Axin is depleted in 293T cells. Panels on the right represent tracings from the autoradiograph on the left, showing Wnt-dependent stabilization of proteins (lanes 1 and 2), but no significant changes after Wnt treatment when Axin was depleted (lanes 3 and 4). Coomassie brilliant blue (CBB) staining serves as an equal loading control. This experiment suggests that disruption of Wnt-signalosome formation (Bilic et al., 2007) and inhibition of the subsequent GSK3 sequestration caused by the depletion of Axin abolishes the Wnt-induced stabilization of protein half-life.

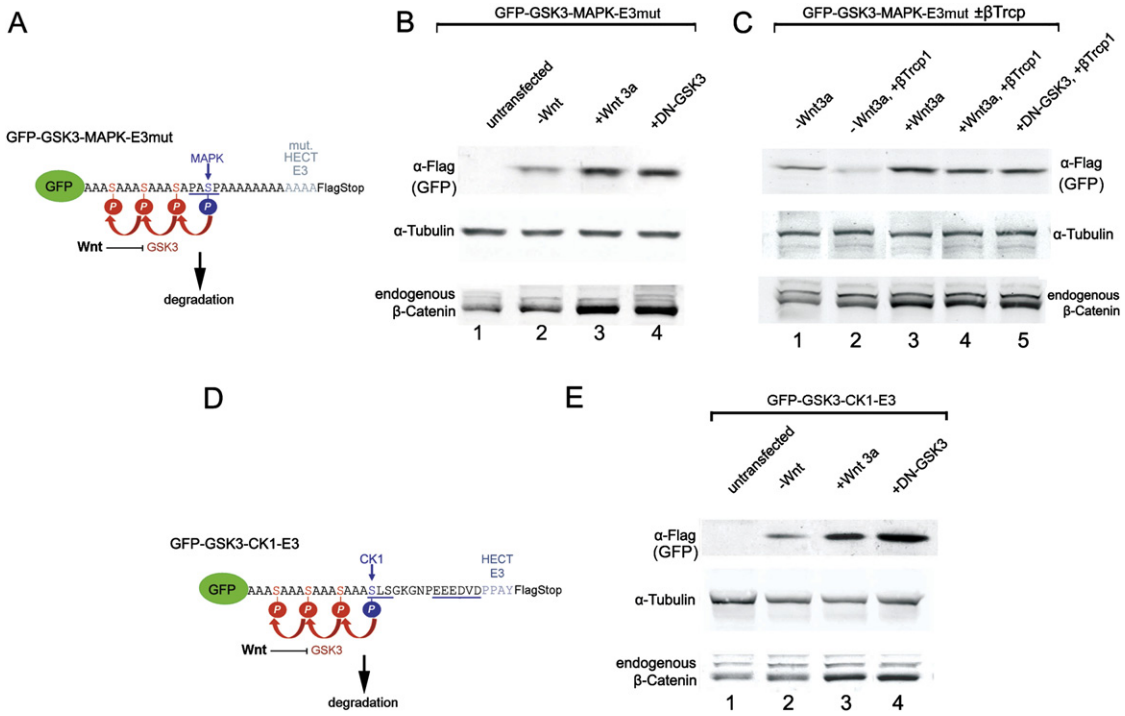

Figure S7. The Wnt Responsiveness of a Reporter Green Fluorescent Protein Is Caused by Its GSK3 Phosphorylation Sites, Related to Figure 6

(A) Diagram introducing the Wnt reporter protein lacking the HECT E3 ligase-binding domain (GFP-GSK3-MAPK-E3mut).

(B) In western blots, the GFP-GSK3-MAPK-E3mut protein was found to be stabilized by Wnt3a treatment or cotransfection with DN-GSK3 (He et al., 1995). This experiment shows that although the E3 polyubiquitin ligase recognition site helps (compare to Figure 6C), it is not essential for Wnt stabilization. In the absence of the PPXY motif, the phosphorylated protein may still be recognized by other E3 ligases, such as βTrcp. β-Catenin serves as an endogenous control for the effectiveness of the Wnt treatment, and α-Tubulin as loading control.

(C) βTrcp overexpression significantly decreased the stability of the GFP-GSK3-MAPK-E3mut protein in western blots (lane 2). Treatment with Wnt3a conditioned medium or cotransfection with DN-GSK3 prevented the effect of βTrcp on this GFP-sensor protein. This suggests that the GFP-GSK3-MAPK-E3mut protein is a substrate of βTrcp only when phosphorylated on its GSK3 sites.

(D) Design of a Wnt reporter construct containing GSK3 sites primed by Casein kinase 1 (CK1), (GFP-GSK3-CK1). The CK1 recognition site used mimics the human β-Catenin sequence, which is underlined.

(E) Western blot analyses showing that the CK1-primed reporter is stabilized by Wnt3a treatment or DN-GSK3 cotransfection. This indicates that the effects of Wnt do not depend on the priming kinase (the stabilization by Wnt is comparable to that of the MAPK primed construct shown in Figure 6C). It should be noted that while the CK1 construct is likely to be phosphorylated in the destruction complex (which contains CK1 and GSK3), GFP-GSK3-MAPK (Figure 6C) is not expected to.